Engineered coumarin accumulation reduces mycotoxin-induced oxidative stress and disease susceptibility

Alexander Beesley[1], Sebastian F. Beyer[1,b], Verena Wanders[1], Sophie Levecque[1], Sandra Bredenbruch[2], Samer S. Habash[2,a], A. Sylvia S. Schleker[2], Jochem Gätgens[3], Marco Oldiges[3], Holger Schultheiss[4], Uwe Conrath[1] (iD) and Caspar J. G. Langenbach[1,*] (iD)

[1]*Department of Plant Physiology, RWTH Aachen University, Aachen, Germany*

[2]*Department of Molecular Phytomedicine, University of Bonn, Bonn, Germany*

[3]*Department of Bioprocesses and Bioanalytics, Research Center Jülich GmbH, Jülich, Germany*

[4]*BASF Plant Science Company GmbH, Agricultural Center, Limburgerhof, Germany*

Summary

Coumarins can fight pathogens and are thus promising for crop protection. Their biosynthesis, however, has not yet been engineered in crops. We tailored the constitutive accumulation of coumarins in transgenic *Nicotiana benthamiana*, *Glycine max* and *Arabidopsis thaliana* plants, as well as in *Nicotiana tabacum* BY-2 suspension cells. We did so by overexpressing *A. thaliana feruloyl-CoA 6-hydroxylase 1* (*AtF6'H1*), encoding the key enzyme of scopoletin biosynthesis. Besides scopoletin and its glucoside scopolin, esculin at low level was the only other coumarin detected in transgenic cells. Mechanical damage of scopolin-accumulating tissue led to a swift release of scopoletin, presumably from the scopolin pool. High scopolin levels in *A. thaliana* roots coincided with reduced susceptibility to the root-parasitic nematode *Heterodera schachtii*. In addition, transgenic soybean plants were more tolerant to the soil-borne pathogenic fungus *Fusarium virguliforme*. Because mycotoxin-induced accumulation of reactive oxygen species and cell death were reduced in the *AtF6'H1*-overexpressors, the weaker sensitivity to *F. virguliforme* may be caused by attenuated oxidative damage of coumarin-hyperaccumulating cells. Together, engineered coumarin accumulation is promising for enhanced disease resilience of crops.

Introduction

Soybean (*Glycine max*) is a rich source of oil, amino acids, and protein and thus belongs to the economically most important crops on Earth (FAOSTAT, 2019; Hartman *et al*., 2011). The USA, Brazil and Argentina are the major soybean-producing countries providing more than 80% of the global soybean yield (FAOSTAT, 2019). Several diseases threaten soybean production and frequently result in economic losses (Bandara *et al*., 2020; Wrather *et al*., 2010). For example, in Argentina and the USA, the sudden death syndrome (SDS), which is caused by the soil-borne fungus *Fusarium virguliforme*, is a frequent late-season disease of the soybean crop. The fungus infects the root of susceptible seedlings and then invades their vascular tissue. It does, however, not seem to infest aerial parts of the plant (Roy *et al*., 1997; Rupe, 1989). Foliar symptoms appear with a huge delay, often as late as at the beginning of flowering or even later (Roy *et al*., 1997). Disease symptoms comprise interveinal chlorosis and necrosis and, eventually, premature defoliation. The latter is caused by mycotoxins that translocate from the infected root to the aerial parts of the plant (Brar *et al*., 2011; Chang *et al*., 2016). In Argentina, 14% of the soybean yield loss have been assigned to SDS (Wrather *et al*., 2010) and in the USA, between 1996 and 2016, an estimated economic loss of almost 4000 USD per hectare was ascribed to SDS (Bandara *et al*., 2020). These losses classify SDS as one of the most threatening soybean

diseases. Measures to control SDS are limited because SDS-resistant soybean cultivars are unavailable and fungicides often ineffective (Westphal, 2008). SDS frequently coincides with the occurrence of soybean cyst nematodes (SCN; *Heterodera glycines*), raising a huge economic bill to soybean production in the USA and the South Americas (Bandara *et al*., 2020; Koenning and Wrather, 2010; Wrather *et al*., 2010). When *H. glycines* and *F. virguliforme* occur together, SDS often is particularly detrimental (McLean and Lawrence, 1993; Westphal *et al*., 2014; Xing and Westphal, 2006). Thus, generating soybean varieties with dual resilience to *F. virguliforme* and *H. glycines* represents a promising strategy to securing soybean yield.

Scopoletin is a compound in the coumarin class of secondary metabolites and a potent antioxidant (Beyer *et al*., 2019). Because of its antifungal, antibacterial, antiviral, and insect deterrent activity, the coumarin qualifies for providing broad-spectrum pest and disease resistance (Beyer *et al*., 2019; Churngchow and Rattarasarn, 2001; Fay and Duke, 1977; Garcia *et al*., 1995; Gómez-Vásquez *et al*., 2004; Goy *et al*., 1993; Olson *et al*., 1991; Prats *et al*., 2002, 2006; Stringlis *et al*., 2018; Sun *et al*., 2014; Tal and Robeson, 1986; Tripathi *et al*., 2011; Valle *et al*., 1997). Consistently, the endogenous level of scopoletin frequently correlates with the extent of disease susceptibility or resistance in various tobacco cultivars and hybrids, sunflowers and various species in the *Platanus* and *Hevea* genera (Chong *et al*., 2002; El Modafar *et al*., 1995; El Oirdi *et al*., 2010; Garcia *et al*., 1999; Goy

et al., 1993; Prats *et al.*, 2007; Sun *et al.*, 2014). The extent of scopoletin accumulation depends on the genotype, age, organ and physiological condition of the plant. For example, in the roots of *Arabidopsis thaliana* (subsequently referred to as Arabidopsis in this paper), scopoletin presence is constitutive. Further biosynthesis and secretion to the rhizosphere are induced during iron deficiency (Fourcroy *et al.*, 2014; Schmid *et al.*, 2014; Siwinska *et al.*, 2014, 2018) or upon root colonization by beneficial rhizobacteria that trigger an induced systemic resistance (ISR) response (Stringlis *et al.*, 2018). Secretion of simple coumarins contribute to plant tolerance to iron starvation (Fourcroy *et al.*, 2014; Schmid *et al.*, 2014; Schmidt *et al.*, 2014), induces shifts in the composition of synthetic root microbiome communities (Voges *et al.*, 2019) and selectively suppresses soil-borne pathogens while promoting the multiplication of ISR-inducing microbes (Stringlis *et al.*, 2018). By doing so, scopoletin and other coumarins are thought to modulate the composition of the root microbiome to the benefit of the plant. Aerial parts of healthy Arabidopsis plants do not constitutively accumulate scopoletin. In leaves, de novo biosynthesis of scopoletin is rather induced by abiotic (e.g. low temperature, 2,4-dichlorophenoxyacetic acid) and biotic stress (e.g. *F. oxysporum, Phakopsora pachyrhizi*) (Beyer *et al.*, 2019; Döll *et al.*, 2018; Kai *et al.*, 2006). Different from Arabidopsis, soybean leaves do not contain scopoletin even upon inoculation with *P. pachyrhizi* (Beyer *et al.*, 2019).

In Arabidopsis, scopoletin biosynthesis is associated with expression of the *FERULOYL-CoA 6-HYDROXYLASE 1* (*F6′H1*) gene (Beyer *et al.*, 2019; Kai *et al.*, 2008; Schmid *et al.*, 2014). *AtF6′H1* encodes a 2-oxoglutarate-dependent dioxygenase catalysing the *ortho*-hydroxylation of feruloyl-CoA to 6-hydroxyferuloyl-CoA (Kai *et al.*, 2008). Despite inactivity of recombinant F6′H1 towards the esculetin precursor caffeoyl-CoA and several other potential phenylpropanoid substrates, esculetin and esculin accumulation in the roots of Arabidopsis wild-type plants has been reported to depend on *F6′H1* (Ziegler *et al.*, 2017). In light-protected organs, such as roots, the isomerization and lactonization of feruloyl-CoA depends on coumarin synthase (COSY) (Vanholme *et al.*, 2019). *In planta*, scopoletin may be further metabolized, e.g. to fraxetin and sideretin (Rajniak *et al.*, 2018; Siwinska *et al.*, 2018) or it is glycosylated by UDP-glycosyltransferases (UGT's) (Chong *et al.*, 2002; Hino *et al.*, 1982; Lim *et al.*, 2003). Scopolin is the glucoconjugate of scopoletin and predominantly accumulates in the vacuole (Taguchi *et al.*, 2000). Different from scopoletin, scopolin has no noticeable antioxidant activity and does not inhibit the intracellular accumulation of reactive oxygen species (ROS; Beyer *et al.*, 2019). It also does not inhibit the germination of, for example, *P. pachyrhizi* spores (Beyer *et al.*, 2019). However, scopolin inhibits the formation of germ tubes of *Sclerotinia sclerotiorum* and halts hyphal growth of *Alternaria alternata* at doses similar to those of active scopoletin (Li and Wu, 2016; Prats

et al., 2006). These findings indicate that scopolin may also exert a direct protective function, at least in some plant–fungus interactions. Alternatively, or in addition, scopolin pools in the vacuole may serve as a reservoir for scopoletin that may quickly be released by scopolin-hydrolysing β-glucosidases after cellular collapse, e.g. after attack from microbial pathogens, nematodes, or chewing insects. Apart from its direct plant protective properties, scopoletin has been suggested to indirectly contribute to plant disease resistance by suppressing the biosynthesis of fungal virulence factors such as mycotoxins (Gnonlonfin *et al.*, 2011). Increased scopoletin content may also augment the nutraceutical value of plant-derived products due to its manifold beneficial properties to human health which include its antidiabetic, anti-inflammatory, anticancer, and anti-obesity activity (Chang *et al.*, 2015; Ding *et al.*, 2008; Ham *et al.*, 2016; Li *et al.*, 2015).

In this work, we explored the feasibility of *AtF6′H1*-overexpression for constitutive accumulation of simple coumarins, particularly scopoletin and scopolin, in transiently transformed *Nicotiana benthamiana* and in stably transformed Arabidopsis and soybean plants, and in tobacco BY-2 culture cells. We also evaluated the possible effect of *AtF6′H1*-overexpression on various plant–pathogen interactions. We show that homologous and heterologous overexpression of *AtF6′H1* mainly leads to constitutive, but differing, accumulation of scopoletin and scopolin between species, organs and compartments. An elevated level of coumarin glycosides in Arabidopsis roots enhanced the resistance to *H. schachtii*. Constitutive accumulation of coumarins in soybean increased the tolerance to SDS associated with increased capacity of *AtF6′H1*-overexpressing cells for buffering excessive mycotoxin-induced ROS accumulation. Engineered coumarin biosynthesis may, therefore, be utilized for increasing the antioxidant capacity and thereby reducing the stress susceptibility of crops.

Results

Heterologous and transient overexpression of *AtF6′H1* in *N. benthamiana* causes scopoletin accumulation

As the first step towards understanding whether expression of *AtF6′H1* suffices for gaining coumarin biosynthesis in another plant species, we transiently overexpressed *AtF6′H1* and different N- or C-terminal fusions of the protein with GFP (green fluorescent protein), RFP (red fluorescent protein) or FLAG in *N. benthamiana*. We then analysed scopoletin abundance, scopoletin fluorescence in UV light, transgene expression and fusion protein accumulation and localization in transformed leaves. Independent of the N- or C-terminus of F6′H1 being translationally fused to a protein tag, transient overexpression of *AtF6′H1* caused strong accumulation of scopoletin in *N. benthamiana* (Figure 1a). Quantitative RT-PCR, immunoblotting analysis and/or fluorescence detection confirmed the

Figure 1 Transient overexpression of *AtF6′H1* causes scopoletin accumulation in *N. benthamiana*. Scopoletin (a) and *AtF6′H1* mRNA transcript (b) in *N. benthamiana* leaves overexpressing *AtF6′H1* or C- or N-terminal fusions of *AtF6′H1* with GFP, RFP or FLAG controlled by the constitutive CaMV *35S* promoter. P19 silencing inhibitor was co-expressed in all cases. Expression of P19 only served as negative control. Shown are means ± SD of three independent experiments at 3 days after transient transformation. (c) Photos of transiently transformed leaves with characteristic fluorescence of scopoletin (in UV light; upper panel), GFP (middle panel) and RFP (lower panel). (d) *AtF6′H1-GFP* co-localizes with cytoplasmic RFP in transiently transformed epidermal cells of *N. benthamiana*. GFP and RFP fluorescence were analysed by confocal laser scanning microscopy. (e, f) Accumulation of GFP and RFP and fusions of both fluorescent proteins and FLAG with AtF6′H1 was verified by SDS-PAGE and immunodetection using antibodies specific to GFP, RFP and FLAG.
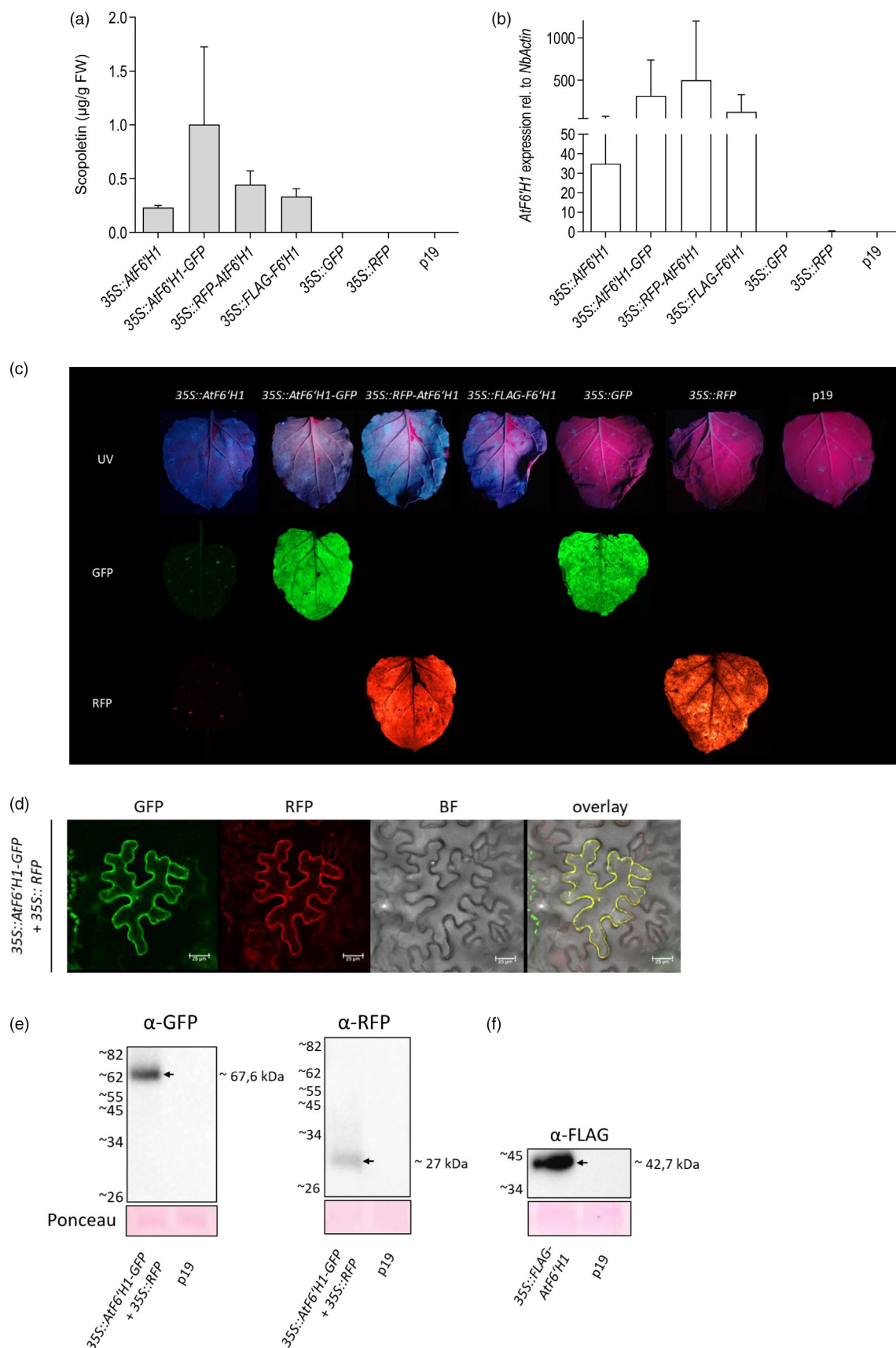
expression of *AtF6'H1* and its fusion DNA constructs only in leaves transformed with the respective transgene-encoding construct but not in p19-expressing controls (Figure 1b,d–f). In UV light, *AtF6'H1*-overexpressing and scopoletin-accumulating leaves displayed fluorescence, whereas control construct-transformed leaves expressing GFP, RFP or the silencing inhibitor p19 alone were neither fluorescent nor did they synthesize detectable amounts of scopoletin (Figure 1a,c). Depending on the DNA construct used, scopoletin levels in *AtF6'H1*-expressing leaves varied from 0.23 to 1 µg/g FW at 3 days after transformation (Figure 1a). Confocal microscopy of leaves transiently co-overexpressing *AtF6'H1-GFP* and *RFP* confirmed the predicted localization of F6'H1 (Softberry.com; ProtComp Version 9.0: cytoplasmic with a score of 8.2) to the cytoplasm (Figure 1d).

Stable overexpression of *AtF6'H1* causes constitutive but varying spatial accumulation of scopoletin and scopolin among different organs of Arabidopsis and soybean

Next, we analysed the accumulation of coumarins in independent transgenic events of Arabidopsis (accession Col-0) and soybean (cultivar W82) stably overexpressing *AtF6'H1* or *FLAG-AtF6'H1*, respectively. Among simple coumarins other than scopoletin and scopolin, we only detected low concentrations of esculin in roots and leaves of transgenic plants (10–100-fold less than scopolin, Figure S2). We therefore focused our analysis on scopoletin and scopolin. Accumulation of the coumarins and fluorescence of leaves were similar in the different transgenic events of a same species. However, pronounced differences were seen between transgenic Arabidopsis and soybean. Arabidopsis leaves displayed strong scopoletin fluorescence in UV light no matter whether the adaxial or abaxial side of the leaf was inspected (Figure 2a). In contrast, only the abaxial side of transgenic soybean leaves displayed strong fluorescence in UV light, whereas the fluorescence of the upper leaf side was only slightly enhanced when compared to the untransformed controls (Figure 2b). In both Arabidopsis and soybean, fluorescence was most intense in leaf veins and trichomes (Figures 2b and S1). Consistently, the scopolin concentration was up to 5-fold greater in leaves of Arabidopsis than soybean with a maximum of ~370 µg/g FW and ~80 µg/g FW, respectively (Figure 2c). The scopoletin content was similar among all analysed leaves of transgenic Arabidopsis and soybean events with average levels of ~3 µg/g FW. The identity of both scopoletin and scopolin was confirmed by HPLC (high performance liquid chromatography) and GC–MS (gas chromatography–mass spectrometry) analysis (Figure S2). No or only little scopoletin and scopolin were detected in leaves of untransformed Arabidopsis and soybean. In roots of *AtF6'H1*-overexpressing Arabidopsis, scopoletin (8–9 µg/g FW) and scopolin (440–490 µg/g FW) levels were much higher than in roots of transgenic soybean (~0.5 µg/g FW scopoletin and ~25 µg/g FW scopolin) (Figure 2c). Consistent with the generally higher coumarin abundance in transgenic Arabidopsis than soybean leaves and roots, scopoletin and scopolin levels of Arabidopsis seeds also exceeded those in soybean seeds by ~10–20-fold (Figure S3). To our surprise, the distribution of scopoletin and scopolin in aboveground and belowground organs of transgenic plants of both species was opposite. Scopoletin and scopolin levels were much higher in roots than in the shoot of Arabidopsis, whereas in soybean, the level of the two coumarins was greater in the shoot than in the root (Figure 2c). Neither in Arabidopsis nor soybean any obvious alterations of phenotype due to *AtF6'H1* overexpression was seen regarding plant growth and development (Figure S4).

Total scopoletin content is highest within cells

We next used *N. tabacum* BY-2 suspension cells stably over-expressing *AtF6'H1* to analyse the cellular distribution of scopoletin and scopolin. In contrast to untransformed BY-2 culture cells, transgenic cells, and their growth medium both displayed characteristic blue fluorescence in UV light (Figure 3a). As in organs of intact plants, in transgenic BY-2 cells, scopoletin predominantly accumulated in its glycosylated scopolin derivative. Approximately 77% of the total scopoletin (free and glycosylated) of culture cells were attributed to scopolin which exclusively accumulated inside the cells (Figure 3b). We never detected scopolin in the culture medium of cells. In contrast, scopoletin was more abundant in the medium than in the cells (Figure 3b).

Upon cellular damage, scopolin is quickly hydrolysed to scopoletin

To quantify the time required for the conversion of supposedly vacuole-localized scopolin to scopoletin by glucosidases (Ahn et al., 2010), we analysed the kinetics of scopolin hydrolysis upon decompartmentalization by simply grinding the leaves. Tissue homogenization is making scopolin available as a substrate to, for example, beta-glucosidase. While scopolin accounted for almost 90% of the total scopoletin content in undamaged soybean leaves, its content quickly decreased to nearly 50% within 1 h after grinding. The scopoletin content increased correspondingly (Figure 4a). In Arabidopsis, however, the initial concentration of scopolin made up 97% of the total scopoletin content. Of the scopolin content in Arabidopsis leaves, 29% was converted to scopoletin within 1 h after tissue grinding the tissue (Figure 4b). Thereafter, scopolin hydrolysis to scopoletin slowed down. At 24-h post-tissue disruption (hpt), more than ~60% and 90% of the initial scopolin had been hydrolysed to scopoletin in the samples from Arabidopsis and soybean, respectively (Figure 4a,b). Thus, upon cellular damage intracellular scopolin seems to be quickly converted to scopoletin.

Scopolin hyperaccumulation in Arabidopsis reduces susceptibility to *H. schachtii*

Because scopoletin and scopolin support plant health and as their concentration was highest in the roots of transgenic Arabidopsis plants, we analysed whether transgenic plants over-accumulating the two coumarins would better ward of root pathogens. Thus, we investigated the extent of susceptibility of the Arabidopsis wild type, *f6'h1* mutant and *F6'H1* overexpressor to the root-attacking beet cyst nematode (BCN) *H. schachtii*. We found that the number of developed female nematodes at the roots seemed to be similar among all genotypes tested when these accumulated <200 µg scopolin per gram root FW. Infection rates on roots containing <200 µg/g scopolin ranged from 2.5 to 17 females per plant (Figure 5a). Within this group of plants, the *f6'h1* mutant which did not accumulate detectable amounts of scopolin in the root seemed to be more susceptible than the wild type with varying amounts of scopolin ranging from 2 to 15 µg/g FW. Strikingly, an apparent and statistically significant reduction in the infection rate of female and male nematodes was seen for the *F6'H1* overexpressor with more than 200 µg scopolin per gram root FW (Figures 5b and S5). Thus, increased levels of coumarin glycosides in Arabidopsis roots coincided with reduced susceptibility to *H. schachtii*. Because low amounts of esculin were detectable in roots of transgenic Arabidopsis plants (Figure S2), other coumarins may also contribute to the observed phenotype.
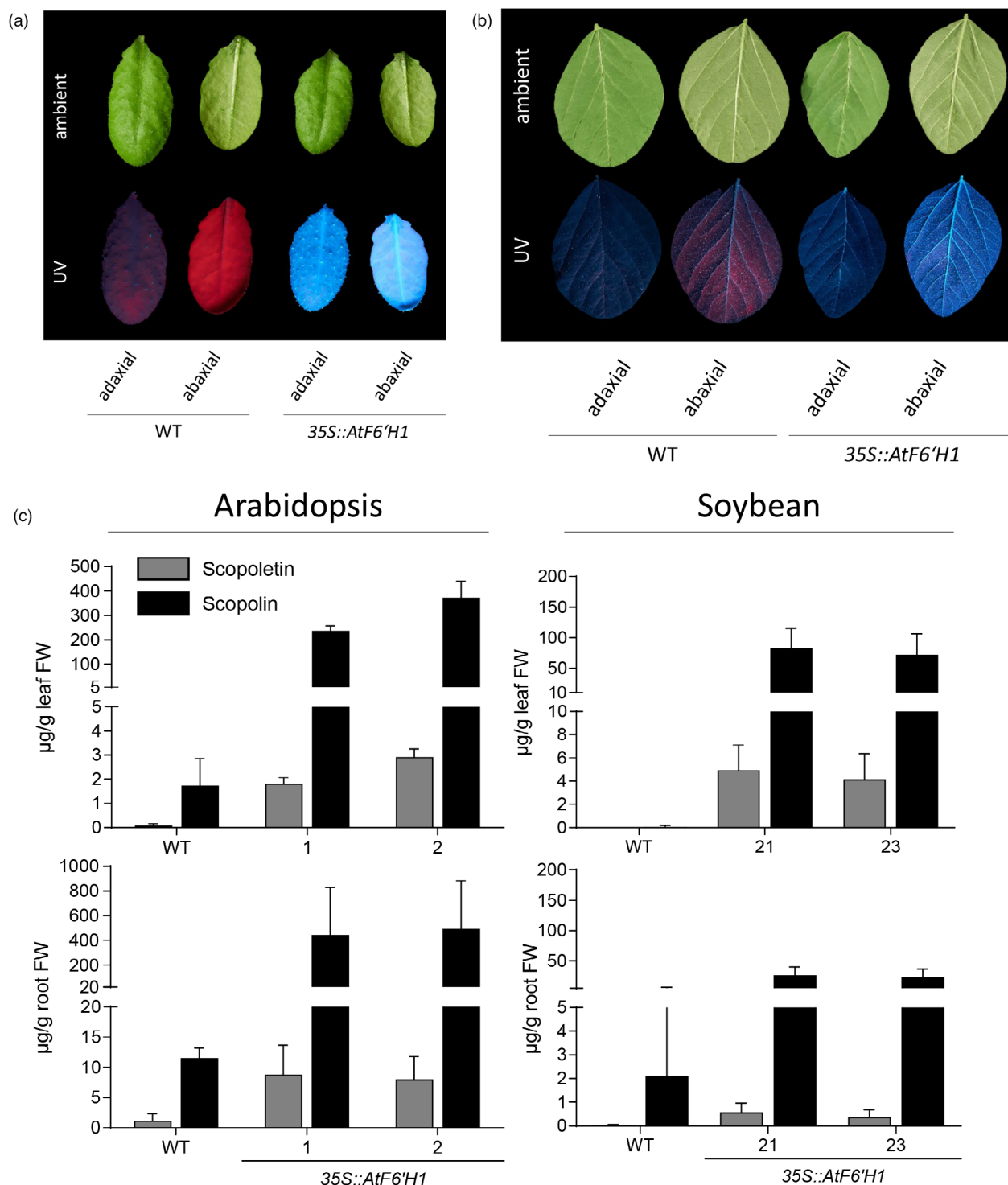
Figure 2 Stable overexpression of *AtF6′H1* in Arabidopsis and soybean results in constitutive coumarin accumulation. Representative photos of adaxial and abaxial sides of detached leaves of Arabidopsis (a) and soybean (b) wild-type and *AtF6′H1*-overexpressing transgenic lines were inspected in ambient or UV light. Only the transgenic plants showed characteristic blue fluorescence of leaves in UV light. (c) Scopoletin and scopolin content in roots and leaves of wild-type Arabidopsis (left panel) and soybean (right panel) and two independent events overexpressing *AtF6′H1*, respectively. Coumarin concentration in methanolic extracts of 3-to-6-week-old plants was quantified by HPLC. Shown is the average + SD of three independent experiments.

Overexpression of *AtF6′H1* induces the SDS tolerance of soybean

Next, we evaluated the interaction of untransformed and *AtF6′H1*-overexpressing soybean plants with *F. virguliforme*.

Before inoculation, no obvious difference was seen between the roots of the two genotypes of plant. Fourteen days after inoculation, the root of both non-transgenic and transgenic plants showed rotting indicating successful *F. virguliforme* infection (Figure 6a). The infected roots were brownish, less
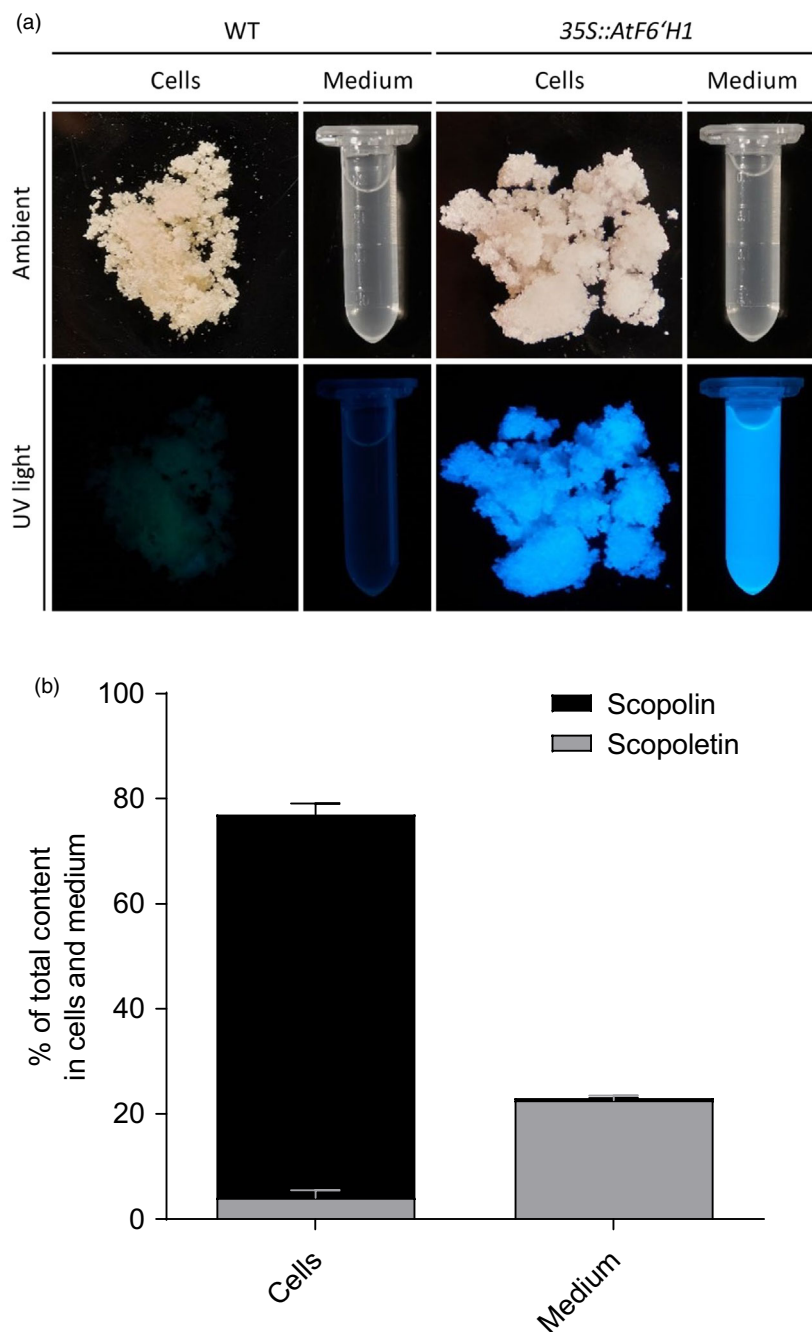
Figure 3 Scopoletin and scopolin mainly accumulate within the cells. (a) *AtF6'H1*-expressing tobacco BY-2 cells, but not the untransformed wild type, and their culture medium fluoresce in UV light. Tobacco BY-2 cells were separated from the growth medium by vacuum filtration at 7 days after subculture. Cells and medium individually inspected in ambient and UV light. (b) Scopoletin and scopolin content of *AtF6'H1*-overexpressing BY-2 cells and their culture medium relative to the total amount of scopoletin and scopolin in the batch culture. Average values and SD of three technical replicates are shown.

dense, and they apparently produced less biomass than non-infected roots (Figure S6). However, no obvious phenotypic differences were observed between roots of non-transgenic and *AtF6'H1*-overexpressing plants (Figure S6). *F. virguliforme* infection of roots severely affected shoot biomass of both genotypes as well (Figure 6b). However, the reduction of shoot biomass was significantly lower for the two independent *AtF6'H1*-transgenic soybean events (~40% decrease) when compared to the wild type (~50% decrease). To analyse, whether the reduced SDS severity of the transgenic plants resulted from diminished root colonization, we determined the abundance of *F. virguliforme* DNA in infected roots. Although, fungal DNA abundance was slightly lower in *F. virguliforme*-infected roots of transgenic plants compared to wild type, the differences were not statistically

significant (Figure 6c). Consistent with these findings, scopoletin in vitro did not significantly inhibit *F. virguliforme* mycelial growth at concentrations lower than 500 µM (Figure S7). These results suggest that overexpressing *AtF6'H1* does not provide direct protection of soybean from *F. virguliforme* but rather attenuates the damage of SDS on the plant. Constitutive coumarin accumulation in soybean thus seems to induce soybean tolerance to SDS disease.

Coumarin accumulation in *AtF6'H1*-overexpressing cells attenuates mycotoxin-induced ROS accumulation and cell death

During infection, many *Fusarium* species produce mycotoxins that may cause oxidative stress and eventually provoke host cell death
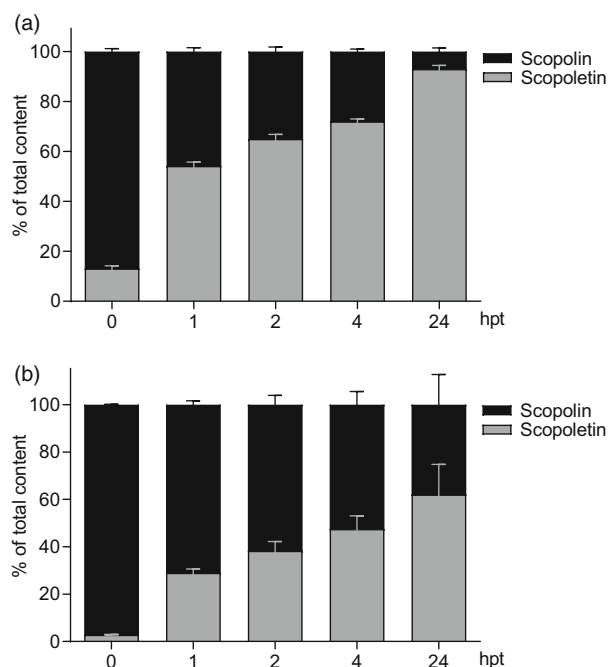
Figure 4 Upon destruction of *AtF6'H1*-overexpressing leaves scopolin is hydrolysed to scopoletin. Leaves of transgenic soybean (a) and Arabidopsis (b) plants were homogenized and analysed for their content of scopolin and scopoletin at the indicated times after tissue disruption (hpt). Average values + SD of three biological replicates are shown.

(Albrecht *et al.*, 1998; Jennings *et al.*, 2001; Singh and Upadhyay, 2014; Yekkour *et al.*, 2015). One such mycotoxin is fusaric acid (FA; 5-butylpicolinic acid). In tomato, the toxin promotes ROS production, lipid peroxidation and cell death (Singh and Upadhyay, 2014). In vitro, scopoletin scavenges ROS (Beyer *et al.*, 2019). To see whether coumarins buffer mycotoxin-induced ROS hyperaccumulation also in planta, we analysed FA-triggered ROS production in soybean. As shown in

Figure 7a, control treatment with water did not notably induce the accumulation of ROS in leaves of wild-type and *AtF6'H1*-transgenic soybean plants. However, a ROS burst was detected in leaves of the wild type after treatment with FA with maximum ROS accumulation at ~25 min post-treatment (Figure 7b). The ROS response to FA was significantly attenuated in leaves overexpressing *AtF6'H1*. Maximum ROS levels in transgenic leaves were about half the levels in leaves of the wild type (Figure 7b,c). To validate the effect of *AtF6'H1* overexpression on the redox state of plants, we also examined ROS accumulation in non-transgenic and *AtF6'H1*-overexpressing BY-2 culture cells in response to FA and the *Fusarium* toxin deoxynivalenol (DON). DON was previously reported to trigger ROS production and cell death in BY-2 cells (Yekkour *et al.*, 2015). Figure 7d reveals that both FA and DON induced a distinct ROS signal in wild-type BY-2 cells. The accumulation of ROS was more enhanced upon treatment with DON (6-fold) than with FA (2-fold) compared to water-treated cells. Neither FA nor DON elicited ROS accumulation in *AtF6'H1*-transgenic, scopoletin-accumulating BY-2 cells (Figure 7d). Consistently, mycotoxin-induced cell death was reduced in transgenic BY-2 cells when compared to the non-transgenic cells (Figure 7e). While the ratio of living to dead wild-type cells decreased enormously after treatment with FA or DON, the viability of transgenic cells was not significantly affected by either of the two mycotoxins (Figure 7f). Together, these data suggest that increasing the content of coumarins in transgenic cells increases the tolerance to mycotoxin-induced oxidative stress and by doing so seems to prevent ROS-induced cell damage and death.

Discussion

Scopoletin occurs in many plant species (Gnonlonfin *et al.*, 2012) in which it is often involved in the response to biotic and abiotic stress (Beyer *et al.*, 2019; Döll *et al.*, 2018; Kai *et al.*, 2006). However, scopoletin is absent from aerial parts of soybean even in stressful condition (Beyer *et al.*, 2019). Numerous studies reported the successful engineering of metabolic pathways to
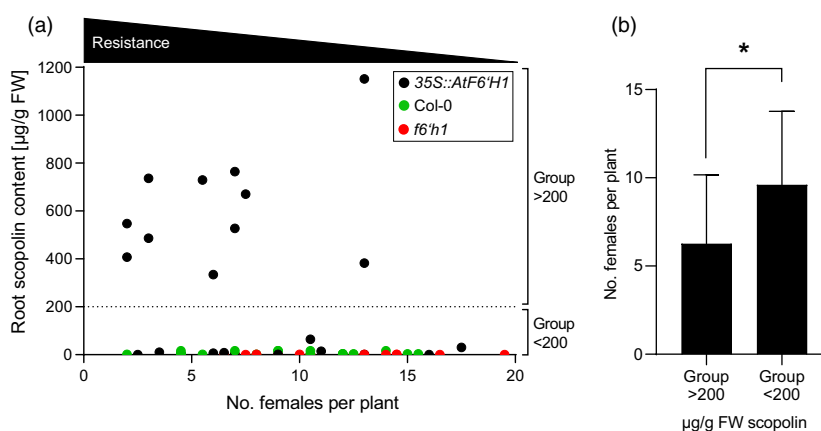
Figure 5 Transgenic Arabidopsis plants with high scopolin levels in root are less susceptible to *H. schachtii*. Wild-type Arabidopsis, *f6'h1* mutants, *AtF6'H1* overexpressors and azygous Arabidopsis plants were grown on agar plates. At 12 days after inoculation with nematodes infection, severity and root content of scopolin were determined. High scopolin levels in roots exceeding 200 μg/g FW coincided with reduced female numbers. Shown are (a) the root scopolin content and infection scores from individual plates with two plants per genotype, respectively. The average infection severity (b) of groups containing more (group >200) or less (group <200) than 200 μg/g FW scopolin in the root. The asterisk marks statistically significant differences between groups >200 and <200 (*t*-test; $P < 0.05$). Three independent experiments with at least four plates (2 plants per plate) per genotype were performed. Data from (a and b) are derived from identical experiments but illustrated in different way.
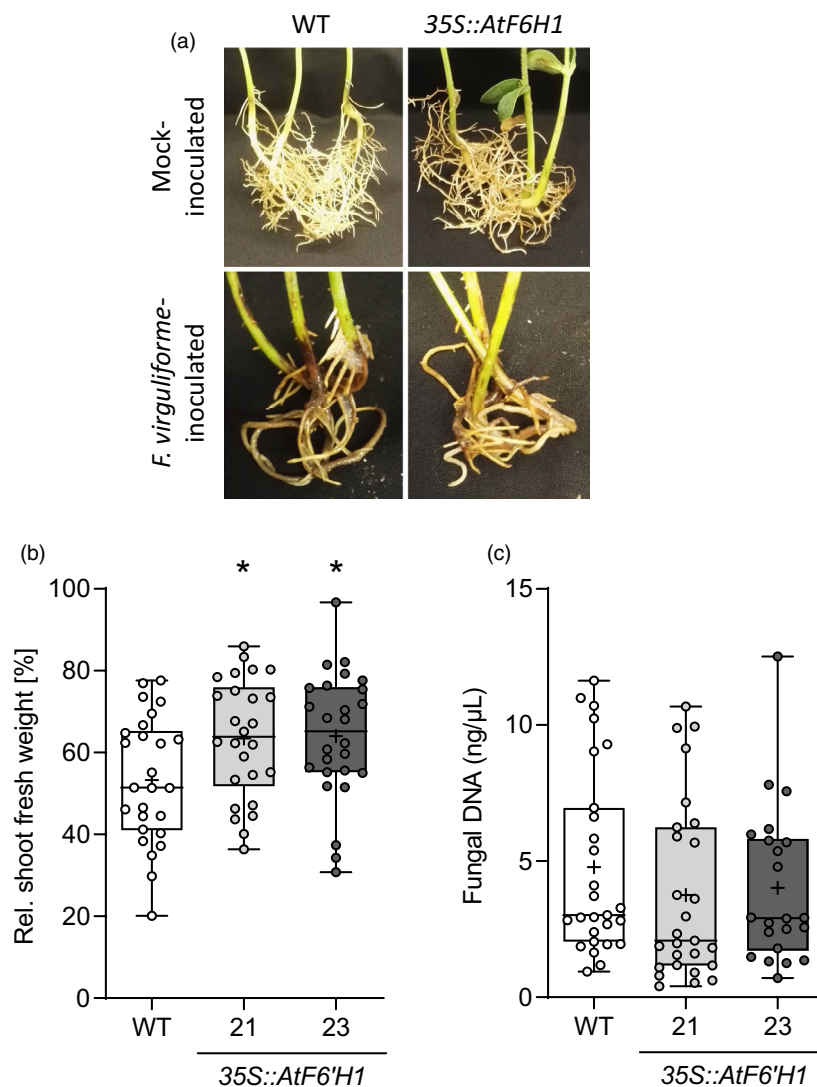
Figure 6 Stable overexpression of *AtF6′H1* in soybean induces SDS tolerance. Wild-type plants and two independent *AtF6′H1*-overexpressing soybean events were hydroponically grown for 7 days prior to root inoculation with spores of *F. virguliforme*. (a) Wild-type and transgenic plants show similar root rotting at 14 days after inoculation. (b) Shoot biomass (fresh weight) of infected wild-type plants or transgenic plants was calculated in comparison with mock-inoculated plants 14 days after inoculation. Shown are min-to-max boxplots with all data points, average values (+) and SD of three independent experiments with nine plants per genotype and treatment. Asterisks indicate significant differences to the wild-type control according to Dunnett's multiple comparisons test with $P \leq 0.05$. (c) Abundance of *F. virguliforme* DNA in infected roots of transgenic and wild-type plants at 14 days after inoculation. DNA was extracted from ≥22 plants per genotype for fungal DNA quantification by qRT-PCR (real-time quantitative reverse transcription PCR). Shown are min-to-max boxplots with all data points, average values (+) and SD of three independent experiments. Differences among wild-type and transgenic plants were not significant according to Dunnett's multiple comparisons test.

accumulate phenylpropanoids (e.g. hydroxycinnamates, flavonoids, isoflavonoids, anthocyanins and stilbenes) in various crops including maize (Liu *et al.*, 2018a,b), rice (Ogo *et al.*, 2013; Shin *et al.*, 2006; Zhu *et al.*, 2017), tomato (Zhang *et al.*, 2015), alfalfa (Deavours and Dixon, 2005), tobacco (Hain *et al.*, 1993; Xie *et al.*, 2006) and soybean (Yu *et al.*, 2003). However, to our knowledge there is no study on the successful engineering of coumarin biosynthesis in crops so far. We took advantage of F6′H1 as the exclusive limiting enzyme for mainly producing

scopoletin from its substrate feruloyl-CoA that is widely abundant in plants. Despite recombinant *AtF6′H1* showing no significant activity towards any tested substrate other than feruloyl-CoA in vitro (Kai *et al.*, 2008), esculetin and esculin concentrations are even significantly lower in roots of the *f6h1* mutant than in roots of the wild type (Ziegler *et al.*, 2017), suggesting at least some minor affinity of F6′H1 for caffeoyl-CoA in vivo to produce esculetin and, following subsequent glycosylation, esculin. Stable overexpression of *AtF6′H1* resulted in coumarin accumulation in

Figure 7 *AtF6′H1* overexpression is associated with decreased ROS accumulation upon mycotoxin exposure. Leaf discs from trifoliate leaves of 19-day-old wild-type or transgenic soybean were floated on (a) water or (b) 30 μg/mL FA. ROS accumulation was recorded over time by luminol-amplified chemiluminescence. Average values ± SD from three independent experiments are shown. (c) Area under the curve (AUC) values (mean ± SEM) were calculated from relative luminescence intensities (RLUs) as measured by the ROS assay for (a) water and (b) FA treatment. Asterisks mark statistical difference relative to the respective treatment in wild-type cells (Sidak's multiple comparisons test, $P < 0.0001$). (d) Treatment with FA and DON induces ROS production in wild-type BY-2 cells but not in *RFP-AtF6′H1*-overexpressing cells. Cells were treated with 30 μg/mL FA or 50 μg/mL DON or water 7 days after subculture and ROS levels quantified by measuring fluorescence intensity in a plate reader following addition of the dye 2′,7′-dichlorofluorescin diacetate (H2DCFDA). Average values and SD from three independent experiments are shown. Asterisks mark statistical difference relative to the respective treatment in wild-type cells (Sidak's multiple comparisons test, $P < 0.0001$). (e) Viability of wild-type and transgenic BY-2 cells was analysed by confocal laser scanning microscopy 4 h after treatment with FA, DON or water (control) and addition of FDA and propidium iodide. (f) Differences were semi-quantitively measured by counting pixels in the respective FDA or PI channels and calculating ratios. Shown are average values and SD from three independent experiments. Asterisks mark statistical difference relative to the respective control treatment (Dunnett's multiple comparisons test, $P < 0.001$).
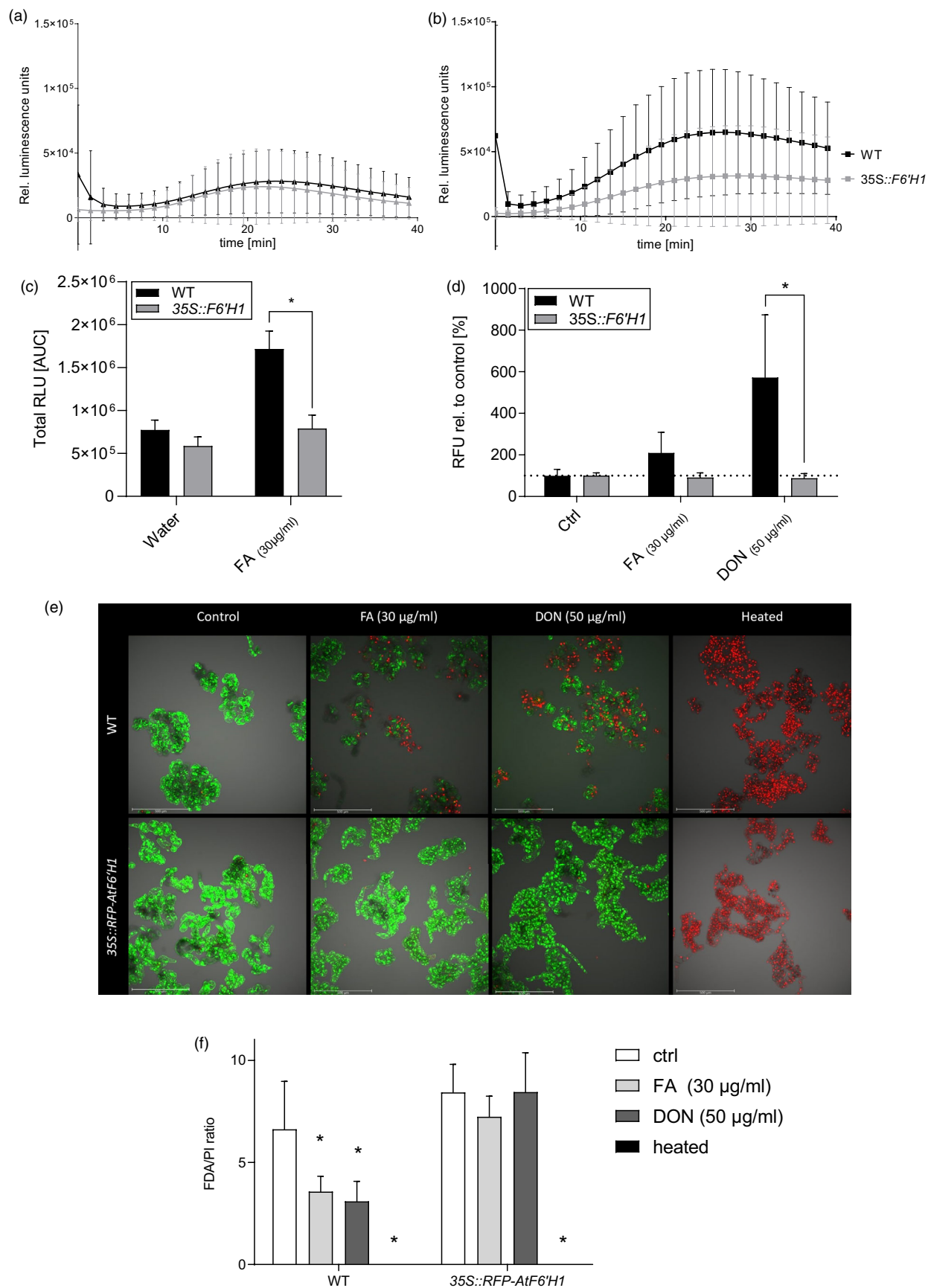
all analysed tissues of the plant species tested (Figures 1 and 2). The lower concentrations of scopoletin and scopolin in transgenic soybean when compared to Arabidopsis plants may be linked to the differential availability of scopoletin's major precursor feruloyl-CoA in the two species. Similarly, the content of the feruloyl-CoA precursor ferulic acid considerably varies among plant species (Zhao and Moghadasian, 2008). Likewise, opposite root-to-leaf ratios of scopoletin and scopolin in transgenic Arabidopsis (~5:1) and soybean (~1:5) may result from different substrate availability in the organs of the two species, different expression levels of the transgene, varying catalytic activity of F6'H1, or differential movement characteristics of scopoletin in Arabidopsis and soybean. In fact, both acropetal and basipetal long-distance transport of flavonoids have been reported for Arabidopsis (Buer et al., 2007). Similarly, UV-induced elicitation of resveratrol biosynthesis caused its accumulation in distal leaves above and below the UV-challenged leaf, indicating bidirectional transport of the polyphenol in grapevine (Wang et al., 2013). For scopolin, a root-to-shoot transport has recently been confirmed in Arabidopsis (Robe et al., 2021). Although unclear whether scopoletin or scopolin is translocated, both have been detected at high concentration in tobacco leaf midveins and Arabidopsis xylem sap (Dieterman et al., 1964; Robe et al., 2021), suggesting that scopoletin may also be transported throughout the plant.

In the analysed transgenic plants and cells, scopoletin levels never exceeded 3–5 µg/g FW but rather accumulated as scopolin (Figures 2 and 3). The distribution of scopoletin and scopolin within transgenic BY-2 cells and in the culture medium was as described before (Okazaki et al., 1982); scopoletin almost exclusively accumulated outside the cells, whereas scopolin was absent from the outside of the cells but accumulated to high levels within cells (Figure 3). Similarly, high scopolin-to-scopoletin ratios (13:1) were recorded in tobacco leaves (Sargent and Skooge, 1960). Due to the potential concentration-dependent toxicity of scopoletin not only for microbes but also for plant cells (Graña et al., 2017), glycosylation of scopoletin and translocation of scopolin to the vacuole likely serve as a mechanism of scopoletin tolerance. Free extracellular scopoletin is a known substrate of peroxidases that oxidize scopoletin in the presence of H_2O_2 (Chong et al., 1999). This confirms scopoletin as a strong antioxidant not only in vitro (Beyer et al., 2019) but also in vivo. Dysregulation of the redox balance by excessive extracellular scopoletin may harm plant cells and cause fitness penalties to the plant. Thus, the rapid uptake of scopoletin from the medium and subsequent glycosylation likely provides a cellular detoxification mechanism when critical concentrations have been reached (Taguchi et al., 2000). However, plants can benefit from a fast provision of the bioactive scopoletin through rapid hydrolysis of the o-glycosidic bond of scopolin. In the incompatible interaction of tobacco with tobacco mosaic virus, in which the hypersensitive response leads to necrotic lesions, scopoletin is quickly released and likely reduces ROS formation (Chong et al., 2002). Also, the accumulation of scopoletin coincides with plant infection from necrotizing fungal pathogens, such as Botrytis cinerea (El Oirdi et al., 2010). Hence, a higher pool of scopolin could potentially enhance the resistance to necrotizing pathogens by providing a pool for the fast scopolin hydrolysis to provide scopoletin. This hydrolysis is being catalysed by ER-localized β-glucosidases (e.g. Arabidopsis BGLUs 21–23) (Ahn et al., 2010) upon the release of scopolin from the vacuole, e.g. when cells are damaged (Figure 4).

BGLU23, which is also known as PYK10 (Nakano et al., 2017), might be particularly interesting. Its expression is induced upon infection with the BCN H. schachtii (Nitz et al., 2001) of Arabidopsis roots where it could be involved in releasing scopoletin from scopolin to counter-infection. High levels of scopolin coincided with reduced numbers of both female and male nematodes developing at the root (Figures 5 and S5). Whether this reduction is caused by scopolin or locally by released scopoletin remains to be elucidated. Previous studies suggested a correlation between nematode-induced ROS accumulation and an increase of antioxidants, such as flavonoids and camalexin (Amjad Ali et al., 2014; Hamamouch et al., 2020; Labudda et al., 2018). Nematodes themselves can also actively modulate plant secondary metabolism, e.g. by secreting chorismate mutase (Vanholme et al., 2009). Yet, to our knowledge, there is no report on the correlation between nematode infection and the accumulation of coumarins in plants. However, recent studies revealed scopoletin to be a potent biocontrol agent against SCN, with scopoletin being active after the treatment of soybean seeds with the compound (Yan et al., 2021). SCNs are in the same genus as H. schachtii and form a disease complex with F. virguliforme, thereby leading to stronger SDS severity of soybean (Westphal et al., 2014; Xing and Westphal, 2006). Increased resistance of coumarin-accumulating soybean lines to SCN may provide a promising strategy for controlling both SCN and F. virguliforme.

Scopoletin inhibited the growth of F. virguliforme in vitro only at high concentrations (Figure S7). This might, at least in part, explain why no effect on root infection severity was observed for transgenic soybean roots accumulating relatively low levels of scopoletin (Figure 6a,c). Consistent with our results, an IC50 of ~1 mM scopoletin was observed in growth inhibition assays with F. solani (Sacc.) Mart. (Peterson et al., 2003), further highlighting the need for high in planta concentrations to directly target the fungal pathogen. Still, plants hyperaccumulating scopoletin were less affected by F. virguliforme and exhibited less fresh weight reduction than wild-type plants (Figure 6b).

Foliar symptoms of Fusarium diseases include water loss of leaves coupled to decreased photosynthesis efficiency (Yan et al., 2018). However, fresh weight reduction of leaves upon detaching, indicative for transpiration-associated water loss, was identical in transgenic lines and wild-type plants (Figure S8), suggesting that increased coumarin concentrations apparently did not directly affect transpiration rate. Instead AtF6'H1 over-expression may provide tolerance to SDS by other means. Apart from its direct antimicrobial activity, scopoletin has been suggested to also indirectly contribute to plant disease resistance by suppressing production of fungal virulence factors like mycotoxins (Gnonlonfin et al., 2011). Consistent with this finding, increasing the content of antioxidant secondary metabolites in plants has been proposed as a potential strategy to improve plant resistance or tolerance, especially for mycotoxin-producing fungi such as Fusarium species (Atanasova-Penichon et al., 2016). The potential of this strategy is further supported by several studies describing the induction of secondary metabolism genes such as those with a role in flavonoid or glyceollin synthesis in response to F. virguliforme infection (Lozovaya et al., 2004; Marquez et al., 2019; Radwan et al., 2011). These often antioxidative metabolites may also be beneficial by improving the capacity of a plant to buffer excessive mycotoxin-induced ROS production and alleviate the associated cellular damage (Yekkour et al., 2015). Indeed, many studies suggest that F. virguliforme mycotoxins induce ROS that are supposed to damage the tissue

through different mechanisms (e.g. Rubisco degradation, membrane degradation and programmed cell death), thereby contributing to foliar symptom development (Abeysekara et al., 2016; Brar et al., 2011; Jin et al., 1996). Increased concentrations of antioxidant coumarins such as scopoletin in plant tissues may therefore contribute to securing plant fitness in stressful conditions by scavenging excessive stress-induced ROS, thereby minimizing chlorophyll degradation, oxidation of lipids, proteins and carbohydrates or other cellular damage associated with oxidative stress (Yu, 1994). Here, we demonstrated that in both *AtF6′H1*-overexpressing soybean plants and BY-2 cells, mycotoxin-induced ROS accumulation was reduced compared to the wild type (Figure 7a–d). The reduction of ROS correlated with decreased cell death in transgenic cells (Figure 7e,f) and might explain the increased tolerance of *AtF6′H1*-transgenic plants to SDS (Figure 6b). Similarly, scavenged ROS accumulation by coumarins in germ tubes of *P. pachyrhizi* antagonized the development of fungal pre-infection structures (Beyer et al., 2019). However, in field trials in Brazil, the susceptibility of *AtF6′H1*-overexpressing lines was slightly, but not significantly, reduced compared to the azygous controls (Figure S9). This finding indicates that the accumulation of coumarins in leaves is not sufficient to provide high levels of protection from SBR (Asian soybean rust). Delivery of spore germination-inhibiting coumarins such as scopoletin to the soybean leaf surface might be needed for an effective coumarin-mediated defence response to the rust fungus. A blueprint of such a defence strategy exists in sunflower. In this plant, increased coumarin secretion to the phylloplane of certain cultivars correlated with their capacity to suppress germination of spores of the sunflower rust fungus *Puccinia helianthi* (Prats et al., 2007).

Due to the reported function of scopoletin as an insect feeding deterrent when mixed with artificial diets (Tripathi et al., 2011), we further compared the interactions between larvae of the generalist insect pest *S. exigua* and soybean wild-type and *F6′H1* overexpressing plants. In a two-choice feeding bioassay, leaf discs of *F6′H1* overexpressing soybean trifoliate leaves were significantly less damaged by feeding larvae than leaves of wild-type controls (Figure S10), confirming coumarins as an insect repellent in planta and further highlighting their broad-spectrum plant-protective potential.

Apart from reducing disease susceptibility, scopoletin may also support the recruitment of beneficial microbes to the rhizosphere, as previously described for Arabidopsis (Lundberg and Teixeira, 2018; Stringlis et al., 2018). Indeed, several reports suggest that an enhanced transcription of *F6′H1* orthologs in soybean roots is associated with the colonization by endophytic microbes such as *Piriformospora indica* and *Bradyrhizobium japonicum* (Bajaj et al., 2018; Libault et al., 2010). In sum, due to its beneficial properties for plants and humans (e.g. through antidiabetic, anti-inflammatory, anticancer and anti-obesity activity) (Chang et al., 2015; Ding et al., 2008; Ham et al., 2016; Li et al., 2015), increasing the concentration of scopoletin and other coumarins in crops may provide a broadly useful agronomic trait. We here showed that engineering this trait is feasible by targeted modulation of the expression of *AtF6′H1* in plants.

Experimental procedures

Plants and fungi

Nicotiana benthamiana seeds were grown in ED73-type soil (Einheitserde Werksverband) in the greenhouse for 4–6 weeks before performing *Agrobacterium*-mediated transient transformation.

Arabidopsis seeds were sown on pipette tips filled with 0.5× Hoagland (1 mM KH2PO4, 1 KNO3, 1 mM MgSO4, 5 mM CaNO3; 50 μM H3BO3, 0.05 μM CoCl2, 0.05 μM CuSO4, 15 μM ZnSO4, 2.5 μM KI, 50 μM MnSO4, 3 μM Na2MnO4, 50 μM Fe3+-EDTA, pH 5) supplemented with agar as previously described (Fourcroy et al., 2014). In short, pipette tips were filled with 0.5× Hoagland supplemented with 0.8% (w/v) agar and placed in a box containing 0.5× Hoagland medium. One seed was placed on each agar-filled pipette tip allowing roots to grow through the tip into the medium below.

For easier separation of root and upper plant parts, soybean plants were grown in 50-mL tubes containing 0.5× Hoagland medium. Growth conditions were maintained at 24 °C and a light period of 16 h.

The suspension cell culture of *N. tabacum* cv. BY-2 (cultivar Bright Yellow-2, BY-2) was grown in a Murashige and Skooge-based medium (4.3 g/L MS-medium, 30 g/L Sucrose, 200 mg/L KH$_2$PO$_4$, 0.2 mg/L 2.4-Dichlorophenoxyacetic acid, 1 mg/L Thiamine-HCL, 100 mg/L Myo-inositol; adjusted to pH 5.8 with 1 M KOH). Cells were subcultured once a week, by pipetting ~5% of cells into fresh medium.

Fusarium virguliforme (Wa1-ss1 (Malvick and Bussey, 2008)) was kindly provided by Dean Malvick (University of Minnesota) and kept on potato dextrose agar (Carl Roth) at ambient temperature and in light deprivation. Spores were harvested by lightly scraping the surface soaked with ddH$_2$O and subsequent filtration through gauze.

Transient transformation of *N. benthamiana* leaves

A. tumefaciens (AGL01) was used for transient transformation of *N. benthamiana* leaves. Agrobacteria were grown and resuspended in infiltration buffer (10 mM MgCl$_2$; 10 mM MES, pH 5.6; 150 μM acetosyringone) to a final OD600 of 1. Agrobacteria containing the silencing suppressor P19 (Voinnet et al., 2003) were grown to a final OD of 0.5 and mixed 1:1 with Agrobacteria containing the gene of interest shortly before being infiltrated into *N. benthamiana* leaves using a syringe. Plants were further kept under long-day conditions (16 h light, 8 h dark, 22 °C) for 3 days, to ensure sufficient accumulation of protein. Leaves were then harvested for further analysis.

Pictures of leaves exposed to UV light (Blak-Ray®, Analytik Jena) were taken using a Sony α 6000 in constant settings. GFP fluorescence was visualized in the ChemiDoc™ MP(BIO-RAD) with blue epi illumination and the 530/28 emission filter. RFP fluorescence was visualized with green epi illumination and 605/50 emission filter. Equal exposure time for all samples ensured comparability.

Cellular localization of fusion proteins

For the analysis of the localization of GFP and RFP fusion proteins, confocal laser scanning microscopy was performed using the TCS SP8 (Leica). Leaf discs were punched out from transformed *N. benthamiana* leaves after 3 days. The leaf discs were then placed on a glass slide for further microscopy, where GFP and RFP fluorescence were inspected to analyse the localization of the fusion proteins. For GFP detection, the excitation wavelength of the argon laser was 488 nm and emission monitored at 500–530 nm. RFP was excited with a diode-pumped solid-state (DPSS) laser at 561 nm and emission detected at 590–625 nm.

Stable transformation of plants and plant cell culture

DNA vectors for stable transformation of plants were generated using Gateway® Cloning as described by the manufacturer (Thermo Fisher). Primers used in this work are listed in Table S2.

For stable Arabidopsis transformation, the floral dip method was used (Clough and Bent, 1998). Therefore, the coding sequence of *AtF6'H1* (AT3G13610) was cloned into the pAMPAT-GWY (kindly provided by Ralph Panstruga) overexpression vector.

Stably transformed soybean plants were provided by the Transformation Facility of the Iowa State University. The construct used for transformation comprised an omega translational enhancer element, a FLAG-protein tag to facilitate detection of the protein and the coding sequence of *AtF6'H1*. The vector pB2GW7 (Karimi et al., 2002) was used as backbone.

BY-2 cell suspension culture was transformed using an established protocol (Graumann and Evans, 2011). For the stable transformation into wild-type BY-2 tobacco cell suspension cells (kindly provided by Fraunhofer IME), the *AtF6'H1* was cloned into the DNA vector pSITE-4NB (Chakrabarty et al., 2007) providing an N-terminal mRFP-tag. Three-day-old cells were co-incubated with transformed agrobacteria for 3 days in the dark at 26 °C on modified MS agar plates (see plants and fungi). After incubation, the cells were washed with medium containing 50 mg/mL timentin and subsequently plated on modified MS agar plates containing 50 mg/mL kanamycin for the selection of transformed cells. Cells were then incubated at 26 °C for 4–6 weeks until callus formation.

Real-time quantitative reverse transcription PCR (qRT-PCR) analysis

The abundance of *AtF6'H1* transcript in transiently transformed *N. benthamiana* leaves was determined by qRT-PCR analysis as described (Beyer et al., 2019). Total RNA was extracted from ground leaf material as described (Chomczynski and Sacchi, 1987). RNA was then transcribed to cDNA according to manufacturer's instructions using 9-mer random oligonucleotides (ThermoFisher Scientific) and RevertAid Reverse Transcriptase (ThermoFisher Scientific). To quantify the transcript abundance, qRT-PCR was performed as per manufacturer's instructions in a BIO-RAD CFX384 REAL-TIME System using iTaq™ Universal SYBR8® Green Supermix (BIO-RAD) and expression normalized to *NbACT2*. The primers used for qRT-PCR are listed in Table S2.

Protein isolation and analysis

Protein was extracted from plant material as previously described (Conrath et al., 1997). Total protein was then fractioned via SDS-PAGE and subsequently transferred to nitrocellulose membrane for immunodetection (Conrath et al., 1997). Primary monoclonal antibodies against GFP and RFP were obtained from Roche and Chromotek, respectively. Antigen–antibody complexes were detected with horseradish peroxidase-linked anti-mouse secondary antibody (Cell Signalling Technology) followed by chemiluminescence detection with Clarity™ Western ECL Substrate (BIO-RAD) in the ChemiDoc™ (BIO-RAD). To check for equal loading Ponceau S (AppliChem), staining was conducted following immunodetection.

Scopoletin and scopolin extraction

Plant material was extracted as described (Beyer et al., 2019). In short, plant material was frozen in liquid nitrogen, ground, weighed and extracted in 90% methanol for 16 h. After centrifugation at full speed for 15 min, the supernatant was evaporated in a concentrator plus (Eppendorf) and the pellet resuspended in 300 µL of methanol. Samples were stored at −20 °C until further analysis.

HPLC analysis

For HPLC analysis, 10 µL sample were separated on a c-18 reverse phase column heated to 40 °C (NUCLEODUR 100-5 C18 ec, MACHEREY-NAGEL). Solvents used for separations were water and acetonitrile both supplemented with 1.5% acetic acid. The flow rate was set at 0.8 mL/min with a gradient (Figure S11) beginning at 10% acetonitrile. The fluorescent compounds scopoletin and scopolin, and esculetin and esculin were detected in the fluorescence detector (RF-20A, Shimadzu) at 365 nm excitation and 470 nm emission and identified by the retention time compared with authentic standards. Retention times were as follows: esculin: ~6.2 min; scopolin: ~6.6 min; esculetin: ~7.9 min; and scopoletin ~11.6 min. Further verification of compound identity was done by inspecting absorption spectra (230–500 nm) in the photodiode array (SPD-M40, Shimadzu). Scopoletin (Tokyo Chemical Industry Co., Ltd.) and scopolin (Aktin Chemicals, Inc.) content was calculated referring to calibration curves prepared with authentic standards. For the complete set-up of HPLC components (all from Shimadzu), see Table S1.

Nematode experiments

f6'h1 T-DNA insertional mutant SALK_132418 (Kai et al., 2008) was obtained from NASC. Homozygous insertion of the T-DNA in the *F6'H1*-gene was confirmed by PCR according to the recommended procedure (http://signal.salk.edu/tdnaprimers.2.html). Seeds of the Arabidopsis wild-type Col-0, *f6'h1* mutant and *F6'H1*-overexpressor plants were surface-sterilized for 30 s in 70% of ethanol followed by 3 min in 1.2% of sodium hypochlorite. Sterile seeds were washed three times, dried on sterile filter paper and stored at 10 °C to promote stratification. Sowing was performed on Knop agar (Sijmons et al., 1991) and subsequently, Arabidopsis was kept at RT and 16 h photoperiod. After 5 days, the scopolin synthesis of the overexpression line was validated via fluorescence and verified. Non-expressive, azygous plants were transferred separately onto fresh Knop agar with two plants per plate. In order to keep conditions consistent among plants, Col-0 and *f6'h1* seedlings of similar size were equally transferred. This resulted in two plants of each genotype growing on each plate. Ten-day-old plants were inoculated along the primary root with 60–70 freshly hatched *H. schachtii* J2s each (Matera et al., 2021). The number of female and male nematodes was evaluated 12 days after inoculation using a Stereo Microscope (Leica, Germany), and mean values of nematode numbers were noted for the two plants on one plate. For scopolin quantification, the two plants on one same plate were pooled, for wild type (Col-0) and *f6'h1*, all plants of one experiment were pooled for coumarin extraction.

Infection of soybean plants with *F. virguliforme*

Seeds of soybeans were germinated for 2 days on water-soaked paper in the dark and then grown for 7 days on moist vermiculite (type Palabora, 3–6 mm; Isola Vermiculite GmbH). The roots of the soybean seedlings were then rinsed with water to remove substrate before placing three seedlings of the same genotype into one 50-mL flacon tube containing 30 mL 0.5× Hoagland solution (see plant and fungal material) either supplemented with 30 million *F. virguliforme* spores or 0.5× Hoagland solution only,

the latter of which served as controls. The plants were then grown in a growth cabinet for 7 days at 17 °C at a photoperiod of 16 h to facilitate infection. After another 7 days at 24 °C and 16 h photoperiod, the fresh weights of the aerial plant parts apart from cotyledons were determined.

The amount of fungal DNA in the root samples was quantified using a qRT-PCR-based method adapted from (Brouwer *et al.*, 2003). Therefore, fungal DNA was extracted and set to 100 ng/µL and then diluted in a 4-fold series with 100 ng/µL soybean DNA. A standard curve was prepared via qRT-PCR using following primers FvTox1.F (5′-GCAGGCCATGTTGGTTCTGTA-3′) FvTox1.R (5′-GCACGTAAAGTGAGTCGTCTCATC-3′) (Wang *et al.*, 2018). Fungal DNA content in infected plant material was calculated using the standard curve (Figure S12).

Mycotoxin-induced ROS in soybean leaf discs and BY-2 cell suspension culture

Mycotoxin-induced ROS in soybean leaves was measured using a luminol-based assay. Trifoliates of 19-day-old soybean plants were used for these experiments. Leaflets were excised, and leaf discs punched out using biopsy punches (5 mm, imtegra GmbH und Co. KG). Leaf discs were then placed in wells of a 96-well-plate filled with 200 µL ddH$_2$O and regenerated over night to avoid injury-related stress responses. After 16 h, the water was replaced with 50 µL of fresh ddH$_2$O and rested for another 30 min. 50 µL of mastermix containing 2-fold elicitor concentration, 40 µM L-012 Luminol, 20 µg/mL HRP, and ddH$_2$O was added, and the plate directly transferred to the plate reader (BertholdTech CENTRO − MikroWin). Chitin served as a positive control and mastermix without elicitor as negative control. Measuring condition were as follows: 1 s/well, 90 s per cycle, mode: well after well, number of cycles: 27.

To indirectly quantify ROS accumulation in BY-2 cells, a H$_2$DCFDA-based assay was performed. Seven-day-old cell suspension cultures were adjusted to an equally packed cell volume and 1 mL of homogenous culture placed into a 24-well plate. Elicitors were added to appropriate concentrations, and the cells incubated while shaking in the dark for 3 h (26 °C, 120 rpm). 200 µL of cell suspension was then transferred to a black NUNC96-well plate (96F NUNCLEON DELTA lack microwell, ThermoFisher Scientific), and 2.5 µg/mL of H$_2$DCFDA was added. Following uptake into the plant cells, endogenous esterases cleave the non-fluorescent H$_2$DCFDA, which is further oxidized to the fluorescent compound 2′-7′-dichlorofluorescin (Beyer *et al.*, 2019). After incubating in the dark for another 30 min, this fluorescence was measured at 483–14 nm excitation and 530–30 nm emission in a CLARIOstar plate reader (BMG Labtech). Relative fluorescence units were set relative to the control to depict the ROS-associated fluorescence.

Mycotoxin-induced cell death in BY-2 culture cells

For cell death visualization and quantification, cells were stained 4 h post-treatment using propidium iodide (PI, 50 µg/mL, 200× stock in ddH$_2$O) and fluorescein diacetate (FDA, 25 µg/mL, 200× stock in acetone). Cells were analysed via confocal laser scanning microscopy (TCS SP Spectral Confocal Microscope, Leica Microsystems) shortly after staining cells for 10–15 min in reaction tubes on a rotating wheel. PI stains nuclei of dead cells, whereas FDA is converted by intracellular esterases resulting in the highly fluorescent fluorescein. The signal resulting from PI-stained nuclei was detected at 561 nm excitation and 579–690 nm emission, and the fluorescein signal of living cells was detected at 488 nm excitation and 523–561 nm emission. Z-stacks of several fields of view were recorded to ensure that cells in all layers were fully visible. To quantify the ratio between PI and FDA signal, the pixel sum in the respective channels was calculated using LAS X software (Leica Microsystems) and background-corrected by subtracting the values from the control. Ratios calculated in this way indirectly represented viability of the cells. Higher values indicate a higher FDA signal compared to the PI signal, thereby showing higher viability of the cells.

Decompartmentalization of leaf cells

Fresh leaves were ground at room temperature and extracted at indicated time points using 1 mL of methanol (100%). Scopoletin and scopolin levels were determined using HPLC analysis, and the ratio subsequently calculated.

Conflict of interest

The authors H.S., U.C. and C.J.G.L. are inventors of project-linked patent WO/2016124515. H.S. is an employee of BASF Plant Science Company GmbH. S.F.B. is an employee of BASF SE. U.C. and C.J.G.L. are employees of AgPrime GmbH.

Accession numbers

AtF6′H1 − AT3G13610.

Author contributions

A.B., S.F.B., S.B., C.J.G.L., U.C., H.S. and A.S.S. designed the experiments. A.B., S.F.B., V.W., S.L., S.B. and S.S.H. performed the experiments. A.B., C.J.G.L. and U.C. wrote the manuscript. J.G. and M.O. performed the GC−MS TOF analysis. All authors revsised the manuscript.

References

Abeysekara, N.S., Swaminathan, S., Desai, N., Guo, L. and Bhattacharyya, M.K. (2016) The plant immunity inducer pipecolic acid accumulates in the xylem sap and leaves of soybean seedlings following *Fusarium virguliforme* infection. *Plant Sci.* **243**, 105–114.

Ahn, Y.O., Shimizu, B.I., Sakata, K., Gantulga, D., Zhou, Z., Bevan, D.R. and Esen, A. (2010) Scopolin-hydrolyzing Beta-glucosidases in roots of Arabidopsis. *Plant Cell Physiol.* **51**, 132–143.

Albrecht, A., Heiser, I., Baker, R., Nemec, S., Elstner, E.F. and Osswald, W. (1998) Effects of the *Fusarium solani* toxin dihydrofusarubin on tobacco leaves and spinach chloroplasts. *J. Plant Physiol.* **153**, 462–468.

Amjad Ali, M., Wieczorek, K., Kreil, D.P. and Bohlmann, H. (2014) The beet cyst nematode *Heterodera schachtii* modulates the expression of WRKY transcription factors in syncytia to favour its development in Arabidopsis roots. *PLoS One*, **9**, e102360.

Atanasova-Penichon, V., Barreau, C. and Richard-Forget, F. (2016) Antioxidant secondary metabolites in cereals: potential involvement in resistance to Fusarium and mycotoxin accumulation. *Front. Microbiol.* **7**, 1–16.

Bajaj, R., Huang, Y., Gebrechristos, S., Mikolajczyk, B., Brown, H., Prasad, R., Varma, A. *et al.* (2018) Transcriptional responses of soybean roots to

colonization with the root endophytic fungus *Piriformospora indica* reveals altered phenylpropanoid and secondary metabolism. *Sci. Rep.* **8**, 1–18.

Bandara, A.Y., Weerasooriya, D.K., Bradley, C.A., Allen, T.W. and Esker, P.D. (2020) Dissecting the economic impact of soybean diseases in the United States over two decades. *PLoS One*, **15**, 1–28.

Beyer, S.F.S.F., Beesley, A., Rohmann, P.F.W.P.F.W., Schultheiss, H., Conrath, U. and Langenbach, C.J.G.C.J.G. (2019) The Arabidopsis non-host defence-associated coumarin scopoletin protects soybean from Asian soybean rust. *Plant J.* **99**, 397–413.

Brar, H.K., Swaminathan, S. and Bhattacharyya, M.K. (2011) The *Fusarium virguliforme* toxin FvTox1 causes foliar sudden death syndrome-like symptoms in soybean. *Mol. Plant Microbe Interact.* **24**, 1179–1188.

Brouwer, M., Lievens, B., Van Hemelrijck, W., Van Den Ackerveken, G., Cammue, B.P.A. and Thomma, B.P.H.J. (2003) Quantification of disease progression of several microbial pathogens on *Arabidopsis thaliana* using real-time fluorescence PCR. *FEMS Microbiol. Lett.* **228**, 241–248.

Buer, C.S., Muday, G.K. and Djordjevic, M.A. (2007) Flavonoids are differentially taken up and transported long distances in Arabidopsis. *Plant Physiol.* **145**, 478–490.

Chakrabarty, R., Banerjee, R., Chung, S.M., Farman, M., Citovsky, V., Hogenhout, S.A., Tzfira, T. et al. (2007) pSITE vectors for stable integration or transient expression of autofluorescent protein fusions in plants: probing *Nicotiana benthamiana*-virus interactions. *Mol. Plant Microbe Interact.* **20**, 740–750.

Chang, H.-X., Domier, L.L., Radwan, O., Yendrek, C.R., Hudson, M.E. and Hartman, G.L. (2016) Identification of multiple phytotoxins produced by *Fusarium virguliforme* including a phytotoxic effector (FvNIS1) associated with Sudden Death Syndrome foliar symptoms. *Mol. Plant Microbe Interact.* **29**, 96–108.

Chang, W.-C., Wu, S.-C., Xu, K.-D., Liao, B.-C., Wu, J.-F. and Cheng, A.-S. (2015) Scopoletin protects against methylglyoxal-induced hyperglycemia and insulin resistance mediated by suppression of advanced glycation endproducts (AGEs) generation and anti-glycation. *Molecules*, **20**, 2786–2801.

Chomczynski, P. and Sacchi, N. (1987) Single-step method of RNA isolation by acid guanidinium thiocyanate-phenol-chloroform extraction. *Anal. Biochem.* **162**, 156–159.

Chong, J., Baltz, R., Fritig, B. and Saindrenan, P. (1999) An early salicylic acid-, pathogen- and elicitor-inducible tobacco glucosyltransferase: role in compartmentalization of phenolics and H_2O_2 metabolism. *FEBS Lett.* **458**, 204–208.

Chong, J., Baltz, R., Schmitt, C., Beffa, R., Fritig, B. and Saindrenan, P. (2002) Downregulation of a pathogen-responsive tobacco UDP-Glc:Phenylpropanoid glucosyltransferase reduces scopoletin glucoside accumulation, enhances oxidative stress, and weakens virus resistance. *Plant Cell*, **14**, 1093–1107.

Churngchow, N. and Rattarasarn, M. (2001) Biosynthesis of scopoletin in *Hevea brasiliensis* leaves inoculated with *Phytophthora palmivora*. *J. Plant Physiol.* **158**, 875–882.

Clough, S.J. and Bent, A.F. (1998) Floral dip: a simplified method for Agrobacterium-mediated transformation of *Arabidopsis thaliana*. *Plant J.* **16**, 735–743.

Conrath, U., Silva, H. and Klessig, D.F. (1997) Protein dephosphorylation mediates salicylic acid-induced expression of PR-1 genes in tobacco. *Plant J.* **11**, 747–757.

Deavours, B.E. and Dixon, R.A. (2005) Metabolic engineering of isoflavonoid biosynthesis in alfalfa. *Plant Physiol.* **138**, 2245–2259.

Dieterman, L.J., Lin, C.Y., Rohrbaugh, L., Thiesfeld, V. and Wender, S.H. (1964) Identification and quantitative determination of scopolin and scopoletin in tobacco plants treated with 2,4-dichlorophenoxyacetic acid. *Anal. Biochem.* **9**, 139–145.

Ding, Z., Dai, Y., Hao, H., Pan, R., Yao, X. and Wang, Z. (2008) Anti-inflammatory effects of scopoletin and underlying mechanisms. *Pharm. Biol.* **46**, 854–860.

Döll, S., Kuhlmann, M., Rutten, T., Mette, M.F., Scharfenberg, S., Petridis, A., Berreth, D.C. et al. (2018) Accumulation of the coumarin scopolin under abiotic stress conditions is mediated by the *Arabidopsis thaliana* THO/TREX complex. *Plant J.* **93**, 431–444.

El Modafar, C., Clérivet, A., Vigouroux, A. and Macheix, J.J. (1995) Accumulation of phytoalexins in leaves of plane tree (Platanus spp.) expressing susceptibility or resistance to *Ceratocystis fimbriata* f. sp. *platani*. *Eur. J. Plant Pathol.* **101**, 503–509.

El Oirdi, M., Trapani, A. and Bouarab, K. (2010) The nature of tobacco resistance against *Botrytis cinerea* depends on the infection structures of the pathogen. *Environ. Microbiol.* **12**, 239–253.

FAOSTAT (2019) Food and Agricultural Organization of the United Nations Statistics Division. http://www.fao.org/faostat/en/#data/QC [accessed 12 November 2020].

Fay, P.K. and Duke, W.B. (1977) An assessment of allelopathic potential in avena germ plasm. *Weed Sci.* **25**, 224–228.

Fourcroy, P., Sisó-Terraza, P., Sudre, D., Savirón, M., Reyt, G., Gaymard, F., Abadía, A. et al. (2014) Involvement of the ABCG37 transporter in secretion of scopoletin and derivatives by Arabidopsis roots in response to iron deficiency. *New Phytol.* **201**, 155–167.

Garcia, D., Sanier, C., Macheix, J.J. and D'Auzac, J. (1995) Accumulation of scopoletin in *Hevea brasiliensis* infected by *Microcyclus ulei* (P. Henn.) V. ARX and evaluation of its fungitoxicity for three leaf pathogens of rubber tree. *Physiol. Mol. Plant Pathol.* **47**, 213–223.

Garcia, D., Troispoux, V., Grange, N., Rivano, F. and D'Auzac, J. (1999) Evaluation of the resistance of 36 Hevea clones to *Microcyclus ulei* and relation to their capacity to accumulate scopoletin and lignins. *For. Pathol.* **29**, 323–338.

Gnonlonfin, G.J.B., Adjovi, Y., Gbaguidi, F., Gbenou, J., Katerere, D., Brimer, L. and Sanni, A. (2011) Scopoletin in cassava products as an inhibitor of aflatoxin production. *J. Food Saf.* **31**, 553–558.

Gnonlonfin, G.J.B., Sanni, A. and Brimer, L. (2012) Review scopoletin – a coumarin phytoalexin with medicinal properties. *CRC. Crit. Rev. Plant Sci.* **31**, 47–56.

Gómez-Vásquez, R., Day, R., Buschmann, H., Randles, S., Beeching, J.R. and Cooper, R.M. (2004) Phenylpropanoids, phenylalanine ammonia lyase and peroxidases in elicitor-challenged cassava (*Manihot esculenta*) suspension cells and leaves. *Ann. Bot.* **94**, 87–97.

Goy, P.A., Signer, H., Reist, R., Aichholz, R., Blum, W., Schmidt, E. and Kessmann, H. (1993) Accumulation of scopoletin is associated with the high disease resistance of the hybrid *Nicotiana glutinosa* x *Nicotiana debneyi*. *Planta*, **191**, 200–206.

Graña, E., Costas-Gil, A., Longueira, S., Celeiro, M., Teijeira, M., Reigosa, M.J. and Sánchez-Moreiras, A.M. (2017) Auxin-like effects of the natural coumarin scopoletin on Arabidopsis cell structure and morphology. *J. Plant Physiol.* **218**, 45–55.

Graumann, K. and Evans, D.E. (2011) Nuclear envelope dynamics during plant cell division suggest common mechanisms between kingdoms. *Biochem. J.* **435**, 661–667.

Hain, R., Reif, H.J., Krause, E., Langebartels, R., Kindl, H., Vornam, B., Wiese, W. et al. (1993) Disease resistance results from foreign phytoalexin expression in a novel plant. *Nature*, **361**, 153–156.

Ham, J.R., Lee, H.I., Choi, R.Y., Sim, M.O., Choi, M.S., Kwon, E.Y., Yun, K.W. et al. (2016) Anti-obesity and anti-hepatosteatosis effects of dietary scopoletin in high-fat diet fed mice. *J. Funct. Foods*, **25**, 433–446.

Hamamouch, N., Winkel, B.S.J., Li, C. and Davis, E.L. (2020) Modulation of Arabidopsis flavonol biosynthesis genes by cyst and root-knot nematodes. *Plan. Theory*, **9**, 253.

Hartman, G.L., West, E.D. and Herman, T.K. (2011) Crops that feed the World 2. Soybean—worldwide production, use, and constraints caused by pathogens and pests. *Food Secur.* **3**, 5–17.

Hino, F., Okazaki, M. and Miura, Y. (1982) Effect of 2,4-Dichlorophenoxyacetic acid on glucosylation of scopoletin to scopolin in tobacco tissue culture. *Plant Physiol.* **69**, 810–813.

Jennings, J.C., Apel-Birkhold, P.C., Mock, N.M., Baker, C.J., Anderson, J.D. and Bailey, B.A. (2001) Induction of defense responses in tobacco by the protein Nep1 from *Fusarium oxysporum*. *Plant Sci.* **161**, 891–899.

Jin, H., Hartman, G.L., Nickell, C.D. and Widbolm, J.M. (1996) Characterization and purification of a phytotoxin produced by *Fusarium solani*, the causal agent of soybean sudden death syndrome. *Phytopathology*, **86**, 277–282.

Kai, K., Mizutani, M., Kawamura, N., Yamamoto, R., Tamai, M., Yamaguchi, H., Sakata, K. et al. (2008) Scopoletin is biosynthesized via ortho -hydroxylation

of feruloyl CoA by a 2-oxoglutarate-dependent dioxygenase in *Arabidopsis thaliana*. *Plant J.* **55**, 989–999.

Kai, K., Shimizu, B.I., Mizutani, M., Watanabe, K. and Sakata, K. (2006) Accumulation of coumarins in *Arabidopsis thaliana*. *Phytochemistry*, **67**, 379–386.

Karimi, M., Inzé, D. and Depicker, A. (2002) GATEWAY vectors for Agrobacterium-mediated plant. *Trends Plant Sci.* **7**, 193–195.

Koenning, S.R. and Wrather, J.A. (2010) Suppression of soybean yield potential in the continental United States by plant diseases from 2006 to 2009. *Plant Heal. Prog.* **11**, 5.

Labudda, M., Różańska, E., Czarnocka, W., Sobczak, M. and Dzik, J.M. (2018) Systemic changes in photosynthesis and reactive oxygen species homeostasis in shoots of *Arabidopsis thaliana* infected with the beet cyst nematode *Heterodera schachtii*. *Mol. Plant Pathol.* **19**, 1690–1704.

Li, C., Han, X., Zhang, H., Wu, J. and Li, B. (2015) Effect of scopoletin on Apoptosis and cell cycle arrest in human prostate cancer cells *in vitro*. *Trop. J. Pharm. Res.* **14**, 611.

Li, J. and Wu, J. (2016) Scopolin, a glycoside form of the phytoalexin scopoletin, is likely involved in the resistance of *Nicotiana attenuata* against *Alternaria alternata*. *J. Plant Pathol.* **98**, 641–644.

Libault, M., Farmer, A., Brechenmacher, L., Drnevich, J., Langley, R.J., Bilgin, D.D., Radwan, O. *et al.* (2010) Complete transcriptome of the soybean root hair cell, a single-cell model, and its alteration in response to *Bradyrhizobium japonicum* infection. *Plant Physiol.* **152**, 541–552.

Lim, E.K., Baldauf, S., Li, Y., Elias, L., Worrall, D., Spencer, S.P., Jackson, R.G. *et al.* (2003) Evolution of substrate recognition across a multigene family of glycosyltransferases in Arabidopsis. *Glycobiology*, **13**, 139–145.

Liu, X., Li, S., Yang, W., Mu, B., Jiao, Y., Zhou, X., Zhang, C. *et al.* (2018a) Synthesis of seed-specific bidirectional promoters for metabolic engineering of anthocyanin-rich maize. *Plant Cell Physiol.* **59**, 1942–1955.

Liu, X., Yang, W., Mu, B., Li, S., Li, Y., Zhou, X., Zhang, C. *et al.* (2018b) Engineering of 'Purple Embryo Maize' with a multigene expression system derived from a bidirectional promoter and self-cleaving 2A peptides. *Plant Biotechnol. J.* **16**, 1107–1109.

Lozovaya, V.V., Lygin, A.V., Li, S., Hartman, G.L. and Widholm, J.M. (2004) Biochemical response of soybean roots to *Fusarium solani* f. sp. *glycines* infection. *Crop Sci.* **44**, 819–826.

Lundberg, D.S. and Teixeira, P.J.P.L. (2018) Root-exuded coumarin shapes the root microbiome. *Proc. Natl. Acad. Sci. USA*, **115**, 5629–5631.

Malvick, D.K. and Bussey, K.E. (2008) Comparative analysis and characterization of the soybean sudden death syndrome pathogen *Fusarium virguliforme* in the northern United States. *Can. J. Plant Pathol.* **476**, 467–476.

Marquez, N., Giachero, M.L., Gallou, A., Debat, H.J., Declerck, S. and Ducasse, D.A. (2019) Transcriptome analysis of mycorrhizal and nonmycorrhizal soybean plantlets upon infection with *Fusarium virguliforme*, one causal agent of sudden death syndrome. *Plant Pathol.* **68**, 470–480.

Matera, C., Grundler, F.M.W. and Schleker, A.S.S. (2021) Sublethal fluazaindolizine doses inhibit development of the cyst nematode *Heterodera schachtii* during sedentary parasitism. *Pest Manag. Sci.* **77**, 3571–3580.

McLean, K.S. and Lawrence, G.W. (1993) Interrelationship of *Heterodera glycines* and *Fusarium solani* in sudden death syndrome of soybean. *J. Nematol.* **25**, 434–439.

Nakano, R.T., Piślewska-Bednarek, M., Yamada, K., Edger, P.P., Miyahara, M., Kondo, M., Böttcher, C. *et al.* (2017) PYK10 myrosinase reveals a functional coordination between endoplasmic reticulum bodies and glucosinolates in *Arabidopsis thaliana*. *Plant J.* **89**, 204–220.

Nitz, I., Berkefeld, H., Puzio, P.S. and Grundler, F.M.W. (2001) Pyk10, a seedling and root specific gene and promoter from *Arabidopsis thaliana*. *Plant Sci.* **161**, 337–346.

Ogo, Y., Ozawa, K., Ishimaru, T., Murayama, T. and Takaiwa, F. (2013) Transgenic rice seed synthesizing diverse flavonoids at high levels: a new platform for flavonoid production with associated health benefits. *Plant Biotechnol. J.* **11**, 734–746.

Okazaki, M., Hino, F. and Kominami, K. (1982) Effects of plant hormones on formation of scopoletin and scopolin in tobacco tissue cultures. *Agric. Biol. Chem.* **46**, 609–614.

Olson, M., Roseland, C. and Craig, R. (1991) Induction of the coumarins scopoletin and ayapin in sunflower by insect feeding stress and effect of coumarins on the feeding of sunflower beetle (Coleoptera, Chrysomelidae). *Environ. Entomol.* **20**, 1166–1172.

Peterson, J.K., Harrison, H.F., Jackson, D.M., Snook, M.E., Snyd, W., Mart, F.S. *et al.* (2003) Biological activities and contents of scopolin and scopoletin in sweetpotato clones. *HortScience*, **38**, 1129–1133.

Prats, E., Bazzalo, M.E., León, A. and Jorrín, J.V. (2006) Fungitoxic effect of scopolin and related coumarins on *Sclerotinia sclerotiorum*. A way to overcome sunflower head rot. *Euphytica*, **147**, 451–460.

Prats, E., Llamas, M.J., Jorrin, J. and Rubiales, D. (2007) Constitutive coumarin accumulation on sunflower leaf surface prevents rust germ tube growth and appressorium differentiation. *Crop. Sci.* **47**, 1119–1124.

Prats, E., Rubiales, D. and Jorrín, J. (2002) Acibenzolar- S -methyl-induced resistance to sunflower rust (*Puccinia helianthi*) is associated with an enhancement of coumarins on foliar surface. *Physiol. Mol. Plant Pathol.* **60**, 155–162.

Radwan, O., Liu, Y. and Clough, S.J. (2011) Transcriptional analysis of soybean root response to *Fusarium virguliforme*, the causal agent of sudden death syndrome. *Mol. Plant Microbe Interact.* **24**, 958–972.

Rajniak, J., Giehl, R.F.H., Chang, E., Murgia, I., Von Wirén, N. and Sattely, E.S. (2018) Biosynthesis of redox-active metabolites in response to iron deficiency in plants. *Nat. Chem. Biol.* **14**, 442–450.

Robe, K., Conejero, G., Gao, F., Lefebvre-Legendre, L., Sylvestre-Gonon, E., Rofidal, V., Hem, S. *et al.* (2021) Coumarin accumulation and trafficking in *Arabidopsis thaliana*: a complex and dynamic process. *New Phytol.* **229**, 2062–2079.

Roy, K.W., Rupe, J.C., Hershman, D.E. and Abney, T.S. (1997) Sudden death syndrome of soybean. *Plant Dis.* **81**, 1100–1111.

Rupe, J.C. (1989) Frequency and pathogenicity of *Fusarium solani* recovered from soybeans with sudden death syndrome. *Plant Dis.* **73**, 581.

Sargent, J.A. and Skooge, F. (1960) Effects of indolacetic acid and kinetin on scopoletin-scopolin levels in relation to grwoth of tobacco tissues in vitro. *Plant Physiol.* **35**, 934–941.

Schmid, N.B., Giehl, R.F.H., Döll, S., Mock, H.-P., Strehmel, N., Scheel, D. *et al.* (2014) Feruloyl-CoA 6'-Hydroxylase 1-dependent coumarins mediate iron acquisition from alkaline substrates in Arabidopsis. *Plant Physiol.* **164**, 160–172.

Schmidt, H., Günther, C., Weber, M., Spörlein, C., Loscher, S., Böttcher, C., Schobert, R. *et al.* (2014) Metabolome analysis of *Arabidopsis thaliana* roots identifies a key metabolic pathway for iron acquisition. *PLoS One*, **9**, 1–11.

Shin, Y.M., Park, H.J., Yim, S.D., Baek, N.I., Lee, C.H., An, G. and Woo, Y.M. (2006) Transgenic rice lines expressing maize C1 and R-S regulatory genes produce various flavonoids in the endosperm. *Plant Biotechnol. J.* **4**, 303–315.

Sijmons, P.C., Grundler, F.M.W., von Mende, N., Burrows, P.R. and Wyss, U. (1991) *Arabidopsis thaliana* as a new model host for plant-parasitic nematodes. *Plant J.* **1**, 245–254.

Singh, V.K. and Upadhyay, R.S. (2014) Fusaric acid induced cell death and changes in oxidative metabolism of *Solanum lycopersicum* L. *Bot. Stud.* **55**, 1–11.

Siwinska, J., Kadzinski, L., Banasiuk, R., Gwizdek-Wisniewska, A., Olry, A., Banecki, B., Lojkowska, E. *et al.* (2014) Identification of QTLs affecting scopolin and scopoletin biosynthesis in *Arabidopsis thaliana*. *BMC Plant Biol.* **14**, 280.

Siwinska, J., Siatkowska, K., Olry, A., Grosjean, J., Hehn, A., Bourgaud, F., Meharg, A.A. *et al.* (2018) Scopoletin 8-hydroxylase: a novel enzyme involved in coumarin biosynthesis and iron-deficiency responses in Arabidopsis. *J. Exp. Bot.* **69**, 1735–1748.

Stringlis, I.A., Yu, K., Feussner, K., de Jonge, R., Van Bentum, S., Van Verk, M.C. *et al.* (2018) MYB72-dependent coumarin exudation shapes root microbiome assembly to promote plant health. *Proc. Natl. Acad. Sci. USA*, **115**, E5213–E5222.

Sun, H., Wang, L., Zhang, B., Ma, J., Hettenhausen, C., Cao, G., Sun, G. *et al.* (2014) Scopoletin is a phytoalexin against *Alternaria alternata* in wild tobacco dependent on jasmonate signalling. *J. Exp. Bot.* **65**, 4305–4315.

Taguchi, G., Fujikawa, S., Yazawa, T., Kodaira, R., Hayashida, N., Shimosaka, M. and Okazaki, M. (2000) Scopoletin uptake from culture medium and accumulation in the vacuoles after conversion to scopolin in 2,4-D-treated tobacco cells. *Plant Sci.* **151**, 153–161.

Tal, B. and Robeson, D.J. (1986) The induction, by fungal inoculation, of ayapin and scopoletin biosynthesis in *Helianthus annuus*. *Phytochemistry*, **25**, 77–79.

Tripathi, A.K., Bhakuni, R.S., Upadhyay, S. and Gaur, R. (2011) Insect feeding deterrent and growth inhibitory activities of scopoletin isolated from

Artemisia annua against *Spilarctia obliqua* (Lepidoptera: Noctuidae). *Insect Sci.* **18**, 189–194.

Valle, T., López, J.L., Hernández, J.M. and Corchete, P. (1997) Antifungal activity of scopoletin and its differential accumulation in *Ulmus pumila* and *Ulmus campestris* cell suspension cultures infected with *Ophiostoma ulmi* spores. *Plant Sci.* **125**, 97–101.

Vanholme, B., Kast, P., Haegeman, A., Jacob, J., Grunewald, W. and Gheysen, G. (2009) Structural and functional investigation of a secreted chorismate mutase from the plant-parasitic nematode *Heterodera schachtii* in the context of related enzymes from diverse origins. *Mol. Plant Pathol.* **10**, 189–200.

Vanholme, R., Sundin, L., Seetso, K.C., Kim, H., Liu, X., Li, J., de Meester, B. *et al.* (2019) COSY catalyses trans–cis isomerization and lactonization in the biosynthesis of coumarins. *Nat. Plants*, **5**, 1066–1075.

Voges, M.J.E.E.E., Bai, Y., Schulze-Lefert, P. and Sattely, E.S. (2019) Plant-derived coumarins shape the composition of an Arabidopsis synthetic root microbiome. *Proc. Natl. Acad. Sci. USA*, **116**, 12558–12565.

Voinnet, O., Rivas, S., Mestre, P. and Baulcombe, D. (2003) An enhanced transient expression system in plants based on suppression of gene silencing by the p19 protein of tomato bushy stunt virus. *Plant J.* **33**, 949–956.

Wang, B., Sumit, R., Sahu, B.B., Ngaki, M.N., Srivastava, S.K., Yang, Y., Swaminathan, S. *et al.* (2018) Arabidopsis novel glycine-rich plasma membrane PSS1 protein enhances disease resistance in transgenic soybean plants. *Plant Physiol.* **176**, 865–878.

Wang, J., Liu, C., Duan, W., Xi, H., Wang, L. and Li, S. (2013) Accumulation and transportation of resveratrol in grapevines treated by ultraviolet-C irradiation. *Life Sci. J.* **10**, 14–27.

Westphal, A., Abney, T.S., Xing, L., Shaner, G. (2008) Sudden death syndrome. *Plant Heal. Instr.* https://doi.org/10.1094/PHI-I-2008-0102-01

Westphal, A., Li, C., Xing, L., McKay, A. and Malvick, D. (2014) Contributions of *Fusarium virguliforme* and *Heterodera glycines* to the disease complex of sudden death syndrome of soybean. *PLoS One*, **9**, e99529.

Wrather, A., Shannon, G., Balardin, R., Carregal, L., Escobar, R., Gupta, G.K. *et al.* (2010) Effect of diseases on soybean yield in the top eight producing countries in 2006. *Plant Health Prog*, **11**, https://doi.org/10.1094/PHP-2010-0102-01-RS

Xie, D.Y., Sharma, S.B., Wright, E., Wang, Z.Y. and Dixon, R.A. (2006) Metabolic engineering of proanthocyanidins through co-expression of anthocyanidin reductase and the PAP1 MYB transcription factor. *Plant J.* **45**, 895–907.

Xing, L.J. and Westphal, A. (2006) Interaction of *Fusarium solani* f. sp. *glycines* and *Heterodera glycines* in sudden death syndrome of soybean. *Phytopathology*, **96**, 763–770.

Yan, J., Xing, Z., Lei, P., Sikandar, A., Yang, R., Wang, Y., Zhu, X. *et al.* (2021) Evaluation of scopoletin from *Penicillium janthinellum* Snef1650 for the control of *Heterodera glycines* in soybean. *Life*, **11**, 1143.

Yan, K., Han, G., Ren, C., Zhao, S., Wu, X. and Bian, T. (2018) *Fusarium solani* infection depressed photosystem performance by inducing foliage wilting in apple seedlings. *Front. Plant Sci.* **9**, 1–10.

Yekkour, A., Tran, D., Arbelet-Bonnin, D., Briand, J., Mathieu, F., Lebrihi, A., Errakhi, R. *et al.* (2015) Early events induced by the toxin deoxynivalenol lead to programmed cell death in Nicotiana tabacum cells. *Plant Sci.* **238**, 148–157.

Yu, B.P. (1994) Cellular defenses against damage from reactive oxygen species. *Physiol. Rev.* **74**, 139–162.

Yu, O., Shi, J., Hession, A.O., Maxwell, C.A., McGonigle, B. and Odell, J.T. (2003) Metabolic engineering to increase isoflavone biosynthesis in soybean seed. *Phytochemistry*, **63**, 753–763.

Zhang, Y., Butelli, E., Alseekh, S., Tohge, T., Rallapalli, G., Luo, J. *et al.* (2015) Multi-level engineering facilitates the production of phenylpropanoid compounds in tomato. *Nat. Commun.* **6**, 1–11.

Zhao, Z. and Moghadasian, M.H. (2008) Chemistry, natural sources, dietary intake and pharmacokinetic properties of ferulic acid: a review. *Food Chem.* **109**, 691–702.

Zhu, Q., Yu, S., Zeng, D., Liu, H., Wang, H., Yang, Z., Xie, X. *et al.* (2017) Development of "Purple Endosperm Rice" by engineering anthocyanin biosynthesis in the endosperm with a high-efficiency transgene stacking system. *Mol. Plant*, **10**, 918–929.

Ziegler, J., Schmidt, S., Strehmel, N., Scheel, D., Abel, S. *et al.* (2017) Arabidopsis transporter ABCG37/PDR9 contributes primarily highly oxygenated coumarins to root exudation. *Sci. Rep.* **7**, 3704.

Supporting information

Additional supporting information may be found online in the Supporting Information section at the end of the article.

Figure S1 Scopoletin mainly accumulates in leaf veins and trichomes of *AtF6′H1*-transgenic Arabidopsis plants. Transgenic Arabidopsis plants were exposed to UV light and photos taken to visualize scopoletin fluorescence.

Figure S2 Confirmation of the identity of scopoletin and scopolin in plant extracts by HPLC and GC–MS analysis. (a) Representative HPLC chromatograms (fluorescence at 365 nm excitation and 470 nm emission) of methanolic extracts from Arabidopsis and soybean wild-type and *AtF6′H*1-overexpressing leaves and roots, authentic standards of esculin, scopolin, esculetin and scopoletin. (b) Verification of scopoletin and scopolin by GC–MS. Shown are the extracted spectra of the peaks of scopoletin and scopolin. Two numbers are given above each peak of the extracted spectra. The upper number indicates the m/z value, the lower represents the intensity.

Figure S3 Scopoletin and scopolin accumulate in seeds of *AtF6′H1*-overexpressing plants. Scopoletin and scopolin accumulate in *AtF6′H1*-transgenic Arabidopsis (a) and soybean (b) seeds but not or only in low amounts in seeds of the respective wild-type controls. Scopoletin and scopolin were quantified by HPLC. Shown are average values and SD from three seed extracts per transgenic event.

Figure S4 No phenotypic differences can be observed between wild-type and coumarin-accumulating soybean plants. Wild-type and *F6′H1*-overexpressing soybean plants were grown in long-day conditions. Photos of six representative plants per genotype were taken 3.5 weeks after sowing. The white scale bar represents 10 cm.

Figure S5 Scopolin levels in roots of *AtF6′H1*-overexpressing Arabidopsis correlate with reduced number of male nematodes at the root. Shown is the average infection severity + SD of groups containing more (group >200) or less (group <200) than 200 μg/g FW scopolin in the root. Differences between groups >200 and <200 are statistically significant (t-test; $P < 0.05$). Three independent experiments with at least four plates (two plants per plate) per genotype were performed.

Figure S6 *AtF6′H1*-overexpressing soybean lines show no obvious sudden death syndrome (SDS) tolerance of roots. Wild-type plants and two independent *AtF6′H1*-overexpressing soybean events were hydroponically grown for 7 days. Plant roots were inoculated with *F. virguliforme* spores. Root biomass (fresh weight) of *F. virguliforme*-infected plants was calculated relative to mock-inoculated plants at 14 days after inoculation. Shown are min-to-max boxplots with all data points, average values (+) and SD of three independent experiments with nine plants per genotype and treatment. No significant differences to the wild type (control) were detected according to Dunnett's multiple comparisons test with $P \leq 0.05$.

Figure S7 Scopoletin, in a dose-dependent manner, reduces *F. virguliforme* biomass production in vitro. Growth medium was supplemented with 0.2% DMSO (control) or the indicated concentration of scopoletin in 0.2% DMSO, inoculated with 4×10^5 *F. virguliforme* spores per mL. Mycelial dry weight was

determined 7 days later. Shown are min-to-max boxplots with all data points, average values (+) and SD of three independent experiments. Significant differences to the negative control are marked with an asterisk (Students *t*-test; *P* < 0.05).

Figure S8 Detached leaves of wild-type and *AtF6′H1*-over-expressing soybean plants exhibit no difference in water loss. Trifoliates from soybean wild-type and transgenic scopoletin-hyperaccumulating plants were detached and exposed to constant light at 26 °C. The relative weight was calculated relative to the fresh weight at time 0 min for each trifolium during 4 h. Mean ± SD shown from three experiments.

Figure S9 *AtF6′H1*-overexpression slightly but non-significantly reduces SBR symptoms at late stages of infection. SBR symptoms were visually scored on three independent *AtF6′H1*-transgenic events of soybean genotype CD215 and azygous control plants at the indicated time points after planting. The experiment was performed in a test plot at Campinas, Brazi,l and consisted of three replicates/plots per event in a randomized design. Shown is the average infection severity of three replicates per event and time point. Differences were not significant according to statistical analysis with a mixed linear model in which the block was random, and test material (event and null) was fixed.

Figure S10 *S. exigua* larvae preferentially feed on wild type, rather than transgenic soybean leaf discs. Twenty-seven leaf discs per indicated genotype were subjected to *S. exigua* feeding. (a) Representative photos of WT (wild type) and transgenic leaf discs 24 h of feeding. (b) The consumed leaf area was assessed and presented relative to the control. Shown are min-to-max boxplots with all data points, average values (+) and SD of three independent experiments. Asterisks indicate statistical difference between samples of WT and transgenic plants (*t*-test, *P* ≤ 0.01).

Figure S11 HPLC gradient. Solvents used were ddH$_2$O and acetonitrile both supplemented with 1.5% acetic acid. The run time was 27 min at a flow rate of 0.8 mL/min.

Figure S12 Standard relationship of fungal DNA dilutions and C$_T$ value in qRT-PCR analysis. Genomic DNA of *F. virguliforme* was mixed with that of soybean and C$_T$ values determined by qRT-PCR.

Table S1 List of HPLC components used in the study. All components were from Shimadzu.

Table S2 List of primers used in the study. Blue colour indicates attB overhangs.